Physica D 34 (1989) 42–89
North-Holland, Amsterdam

ON THE CALCULATION OF QUANTUM MECHANICAL GROUND STATES FROM CLASSICAL GEODESIC MOTION ON CERTAIN SPACES OF CONSTANT NEGATIVE CURVATURE

R. TOMASCHITZ
Sechsschimmelg. 1/21-22, A-1090 Vienna, Austria and KFA Jülich (IFF), D-5170 Jülich, FRG

Received 20 March 1988
Accepted 23 June 1988
Communicated by V.I. Arnol'd

We consider geodesic motion on three-dimensional Riemannian manifolds of constant negative curvature, topologically equivalent to $S \times]0,1[$, S a compact surface of genus two. To those trajectories which are bounded and recurrent in both directions of the time evolution $t \to +\infty$, $t \to -\infty$ a fractal limit set is associated whose Hausdorff dimension is intimately connected with the quantum mechanical energy ground state, determined by the Schrödinger operator on the manifold.

We give a rather detailed and pictorial description of the hyperbolic spaces we have in mind, discuss various aspects of classical and quantum mechanical motion on them as far as they are needed to establish the connection between energy ground state and Hausdorff dimension and give finally some examples of ground state calculations in terms of Hausdorff dimensions of limit sets of classical trajectories.

0. Introduction

Geodesic motion on manifolds of constant negative curvature has often provided – due to the fact that such manifolds sometimes admit analytically very tractable normal forms though the trajectories behave very erratically – interesting examples for various dynamical concepts like ergodicity, entropy, mixing, Bernoulli property etc. (cf. e.g. Anosov [4], Pesin [37]).

In 1956 Selberg [40] and Huber [23] announced a deep connection between the eigenvalues of the Laplace–Beltrami operator (which is the Schrödinger operator as far as quantized geodesic motion is concerned) and the homotopy classes of geodesic trajectories on such manifolds, and they derived for this connection a relation which is nowadays called Selberg's trace formula (cf. e.g. McKean [32]).

This discovery initiated amongst many other things a thorough study of the spectral properties of the Laplace–Beltrami operator, mainly on Riemann surfaces (cf. e.g. [39, 15, 33, 22, 13]) but also on three-dimensional hyperbolic manifolds (cf. [16]). As an offspring of these investigations Patterson [34] derived an extremely interesting relation between the lowest eigenvalue of the Laplace–Beltrami operator and the Hausdorff dimension of a fractal set that emerges at infinity of hyperbolic space as the set of initial and end points of trajectories that are bounded and recurrent in both time directions $t \to +\infty$, $t \to -\infty$. This connection is exact, no kind of semiclassical approximation is involved.

While Selberg's trace in its present form (cf. e.g. [46, 22]) turned out to be numerically not accessible (even in two dimensions cf. [19, 20, 5]), the above-mentioned relation is, and will be used here to determine on some three-dimensional hyperbolic manifolds (i.e. Riemannian manifolds of constant sectional Gauss-

ian curvature $-1/R^2$, R being the curvature radius of hyperbolic space) the energy ground state E_0 via

$$E_0 = \frac{\hbar^2}{R^2 m}\delta_H\left(1 - \frac{\delta_H}{2}\right), \tag{0.1}$$

where $\hbar$ denotes Planck's quantity, m the mass of the geodesically moving particle and δ_H the Hausdorff dimension of the limit set.

The paper is written up as follows: In section 1 we give an elementary geometric description of the hyperbolic manifolds we will deal with (see also section 8), derive their normal forms in three-dimensional hyperbolic space, discuss various aspects of classical geodesic motion on them and explain the origin of the fractal set, whose Hausdorff dimension is involved in (0.1).

To derive formula (0.1) in section 4 we need some facts about the spectral theory of the Schrödinger operator, which we present in sections 2 (resolvent) and 3 (ground state eigenfunction). In sections 5 and 6 we provide practical construction techniques for hyperbolic manifolds and in section 7 a method to localize the limit set and to calculate its Hausdorff dimension.

In the final section 8 we present various examples of hyperbolic manifolds and calculate ground state energies of the quantized geodesic motion on them via Hausdorff dimensions of limit sets of classical trajectories.

1. Hyperbolic manifolds, classical geodesic motion on them and the emergence of a fractal set

The space in which our manifolds are modelled and from which their metric structure is inherited is Poincaré's upper half-space version of hyperbolic geometry: $H^3 := \{(y_1, y_2, y_3) \in \mathbb{R}^3, y_3 > 0\}$, endowed with a Riemannian metric of constant negative curvature $-1/R^2$ (cf. e.g. [3, 8]),

$$ds^2 = \frac{R^2(dy_1^2 + dy_2^2 + dy_3^2)}{y_3^2}. \tag{1.1}$$

Indeed, H^3 is isometric to the standard model of three-dimensional hyperbolic geometry, namely to the upper sheet Q^3 of a two-sheeted hyperboloid in $\mathbb{R}^4$,

$$x_0^2 - \boldsymbol{x}^2 = R^2, \quad x_0 > 0, \quad \boldsymbol{x} := (x_1, x_3, x_3), \tag{1.2}$$

with the pseudo-Euclidean metric of $\mathbb{R}^4$,

$$ds^2 = d\boldsymbol{x}^2 - dx_0^2, \tag{1.3}$$

restricted to it. For explicit formulae for the isometry $Q^3 \leftrightarrow H^3$ see [8] or section 2. The orientation-preserving invariance group of the metric (1.3) on Q^3 is the restricted orthochronous Lorentz group $SO^+(3,1)$, acting on Q^3 by the standard matrix representation, and this group is known to be isomorphic to $SL(2,\mathbb{C})/\{\pm id\}$, the group of two by two complex matrices with determinant 1; the quotient simply means that two matrices differing by an overall sign are identified.

It is evident that $SL(2,\mathbb{C})/\{\pm id\}$ is isomorphic to the group of complex Möbius transformations in the extended complex plane $\mathbb{C} \cup \{\infty\}$: To every matrix $A := \pm\begin{pmatrix} a & b \\ c & d \end{pmatrix}$ in $SL(2,\mathbb{C})/\{\pm id\}$ we associate a

Möbius transformation via

$$z \to Az = \frac{az+b}{cz+d}. \tag{1.4}$$

Every Möbius transformation can be realized by a successive performance of four (or fewer) inversions in circles or straight lines (e.g. [17]). An inversion in a circle in $\mathbb{R}^2$ or an inversion in a sphere in $\mathbb{R}^3$ with center $\boldsymbol{M}$ and radius r is defined as

$$\boldsymbol{x} \to \zeta(\boldsymbol{x}) = \boldsymbol{M} + \frac{r^2}{|\boldsymbol{x}-\boldsymbol{M}|^2}(\boldsymbol{x}-\boldsymbol{M}). \tag{1.5}$$

Observe that

$$(\boldsymbol{x}-\boldsymbol{M})(\zeta(\boldsymbol{x})-\boldsymbol{M}) = r^2. \tag{1.6}$$

In the case of inversion in a straight line in $\mathbb{R}^2$ or a plane in $\mathbb{R}^3$ $\zeta(\boldsymbol{x})$ denotes the mirror image of $\boldsymbol{x}$ with respect to the straight line or the plane.

The complex plane is just the boundary of the hyperbolic half-space H^3, and we can lift the action (1.4) of $\mathrm{SL}(2,\mathbb{C})/\{\pm\mathrm{id}\}$ on $\mathbb{C}$ to H^3 as follows (Poincaré): We choose four or fewer circles or straight lines representing a given Möbius transformation via a succession of inversions, replace them by hemispheres in $H^3 \cup \mathbb{C}$ with the same centers and radii or by half-planes orthogonal to $\mathbb{C}$, and define the lifted (extended) Möbius transformation in $H^3 \cup \mathbb{C} \cup \{\infty\}$ as a succession of inversions in these hemispheres or half-planes. We list also the analytic expression for these lifted transformations (cf. [8]; we use complex notation, $z := y_1 + \mathrm{i}y_2$, $\bar{z} := y_1 - \mathrm{i}y_2$):

$$\begin{aligned} &\gamma\colon H^3 \to H^3, \\ &\gamma\colon (z, y_3) \to \left(\frac{(az+b)(\overline{cz+d}) + ac\bar{y}_3^2}{|cz+d|^2 + |c|^2 y_3^2}, \frac{y_3}{|cz+d|^2 + |c|^2 y_3^2} \right). \end{aligned} \tag{1.7}$$

It is clear from both the definition and the expression (1.7) that the restriction of the lifted transformation to $\mathbb{C} \cup \{\infty\}$ ($y_3 = 0$) is still given by (1.4).

Moreover, the lifted transformations map H^3 bijectively onto itself and preserve the Poincaré metric (1.1). The standard matrix representation $\mathrm{SO}^+(3,1)$ on Q^3 is equivalent to the representation (1.7) of $\mathrm{SL}(2,\mathbb{C})/\{\pm\mathrm{id}\}$, acting via extended Möbius transformations on H^3. We refer to $\mathrm{SL}(2,\mathbb{C})/\{\pm\mathrm{id}\}$ as the orientation-preserving invariance group of three-dimensional hyperbolic space.

The extended Möbius transformations in H^3 inherit some important properties of the two-dimensional ones in the complex plane. Two-dimensional transformations (1.4) map circles and straight lines onto circles and straight lines (cf. e.g. [17]), and the extended transformations map hemispheres in H^3 with centers in the complex plane and half-planes orthogonal to the complex plane again onto hemispheres centered in $\mathbb{C}$ and half-planes orthogonal to $\mathbb{C}$. In order to imagine the action of the lifted transformation in $H^3 \cup \mathbb{C} \cup \{\infty\}$ it is therefore always useful to look at the base circles of the hemispheres resting on the complex plane, which are transformed by (1.4). Just as the two-dimensional transformations (1.4) are bijective, conformal (i.e. angle preserving) maps of $\mathbb{C} \cup \{\infty\}$ onto itself, the extended transformations in H^3 also enjoy these properties.

We need also some facts about geodesic motion in H^3. As a straightforward generalization of free motion in Euclidean space, the Lagrange function for geodesic motion in a curved Riemannian space with line element

$$ds^2 = \sum_{i,j=1}^{3} g_{ij}(x)\,dx_i\,dx_j$$

is given by

$$L = \tfrac{1}{2}m \sum_{i,j=1}^{3} g_{ij}(x)\dot{x}_i\dot{x}_j \equiv E. \tag{1.8}$$

(The overdots denote time derivatives.) The identity means that L is a constant of motion, for the (g_{ij}) are time independent.

In the case of the line element (1.1) we have

$$L = \tfrac{1}{2}m\frac{R^2}{y_3^2}\left(\dot{y}_1^2 + \dot{y}_2^2 + \dot{y}_3^2\right) \equiv E. \tag{1.9}$$

It is clear from this expression that the component of the initial direction in the (y_1, y_2)-plane is left unchanged by the motion; the particle remains always in a half-plane orthogonal to $\mathbb{C}$ determined by the initial direction. Denoting by x and y Cartesian coordinates in this half-plane we have

$$L = \tfrac{1}{2}m\frac{R^2}{y^2}\left(\dot{x}^2 + \dot{y}^2\right) \equiv E. \tag{1.10}$$

As a second constant of motion we have

$$\frac{\partial L}{\partial \dot{x}} = m\frac{R^2}{y^2}\dot{x} \equiv p. \tag{1.11}$$

Combining (1.10) and (1.11) we get

$$E = \tfrac{1}{2}\frac{1}{R^2}\frac{p^2}{m}y^2\left(1 + \left(\frac{dy}{dx}\right)^2\right). \tag{1.12}$$

Solving this equation we see that the geodesics are arcs of semicircles orthogonal to the (y_1, y_2)-plane,

$$(x - x_0)^2 + y^2 = \frac{2ER^2m}{p^2}. \tag{1.13}$$

In the case that $p = 0$ we have instead of (1.13) $x = x_0$, i.e. the trajectories are straight lines perpendicular onto the (y_1, y_2)-plane. To get the time dependence of the motion we have also from (1.10) and (1.11)

$$\left(\frac{dy}{dt}\right)^2 = \frac{2Ey^2}{mR^2} - p^2\frac{y^4}{m^2R^4} \tag{1.14}$$

or

$$y(t) = \frac{R\sqrt{2mE}}{p} \frac{1}{\cosh\left(\frac{\sqrt{2E/m}}{R}(t-t_0)\right)}, \tag{1.15}$$

with

$$y_0 := y(t_0) = \frac{R\sqrt{2mE}}{p} \tag{1.16}$$

if $p \neq 0$ (cf. also (1.13)).

In the case that $p = 0$ we have instead of (1.15)

$$y(t) = y_0 \exp\left(\frac{\sqrt{2E/m}}{R}(t-t_0)\right), \tag{1.17}$$

where y_0 can be chosen freely.

From (1.13), (1.15) and (1.16) we also get

$$\sinh^2\left(\tfrac{1}{2}\frac{\sqrt{2E/m}}{R}(t-t_0)\right) = \frac{(x-x_0)^2 + (y-y_0)^2}{4yy_0}, \tag{1.18}$$

which is p-independent and remains also true for $p = 0$. From (1.8) and (1.10) it is evident that $\sqrt{2E/m}\,(t-t_0)$ is just the hyperbolic distance between (x_0, y_0) and (x, y) in H^3 (x, y are coordinates in a half-plane in H^3 orthogonal to $\mathbb{C}$).

The construction principle of three-dimensional hyperbolic manifolds (hyperbolic means here that they can be endowed with a Riemannian metric of constant negative curvature) in hyperbolic space H^3 is best explained by a two-dimensional Euclidean example:

One can represent a Riemann surface of genus one (a torus) as a square $\mathscr{F}$ in $\mathbb{R}^2$ with vertices $(0,0) - (1,0) - (1,1) - (0,1)$, the sides $(0,0) - (1,0)$ and $(1,0) - (1,1)$ being identified by the Euclidean translation $(x, y) \to (x, y) + (0,1)$ and the other two sides by the translation $(x, y) \to (x, y) + (1,0)$. This torus inherits a Riemannian metric of zero curvature from $\mathbb{R}^2$ by restricting the Euclidean metric $ds^2 = dx^2 + dy^2$ of $\mathbb{R}^2$ to the square. That this metric fits also smoothly on the sides which are identified by the above two transformations is due to the fact that ds^2 is invariant under these transformations and that the square is a fundamental domain for the subgroup Γ of Euclidean translations generated by these two translations. Fundamental domain means here that if we apply all elements of Γ to the square we get a tesselation of $\mathbb{R}^2$ with squares which do not overlap and cover all of $\mathbb{R}^2$.

Every geodesic on the torus $\mathscr{F}_M$, i.e. the unit square $\mathscr{F}$ with identified sides can be obtained by choosing suitably a geodesic s in $\mathbb{R}^2$ and projecting it into $\mathscr{F}$. The projection map π is defined so, that if a square $\gamma(\mathscr{F})$, $\gamma \in \Gamma$, in the tesselation of $\mathbb{R}^2$ contains a piece of the geodesic in $\mathbb{R}^2$, this piece is mapped into $\mathscr{F}$ by γ^{-1}. (Technically speaking, π is the natural projection map of the universal covering space $\mathbb{R}^2$ of $\mathscr{F}_M$ onto $\mathscr{F}_M \cong \mathbb{R}^2/\Gamma$.) So, for example, if we have a straight line s in $\mathbb{R}^2$ that encloses the angle φ with the side $(0,0) - (1,0)$ of $\mathscr{F}$ and $\tan\varphi$ is a rational number then $\pi(s)$ is a closed loop on $\mathscr{F}_M$. If $\tan\varphi$ is irrational the image $\pi(s)$ is dense in $\mathscr{F}$, the trajectory comes arbitrarily close to every point of the torus.

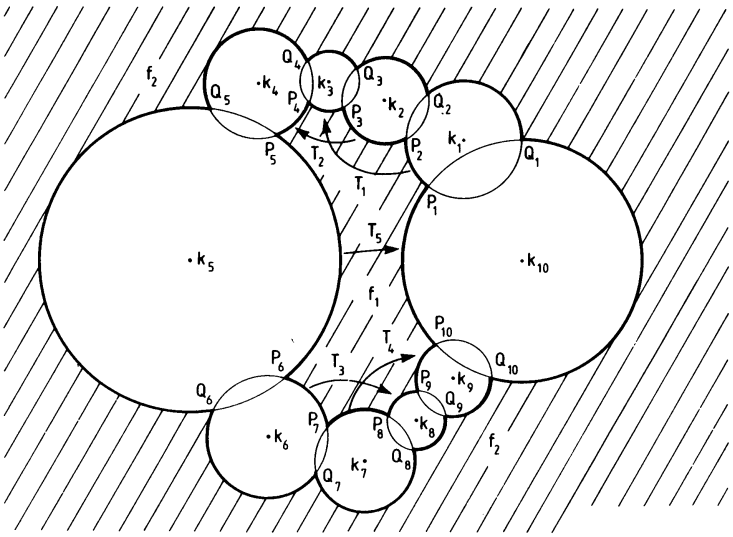

Fig. 1. Identification pattern for the base circles of ten intersecting hemispheres in the plane at infinity of H^3, giving rise to two compact surfaces of genus two (hatched), the boundary components of our hyperbolic manifolds; see sections 1, 5, 8.

Quite analogously to this two-dimensional example we model now manifolds $\mathscr{F}_M$ in H^3 by constructing a domain $\mathscr{F}$ bordered by geodesic planes (domains on hemispheres centered in the complex plane) and by identifying these planes via lifted Möbius transformations, so that we get topologically the desired manifold $\mathscr{F}_M$ (which is in our case homeomorphic to $S \times]0,1[$, S a compact surface of genus two, i.e. a sphere with two handles). $\mathscr{F}$ must be a fundamental domain for the discrete group Γ of lifted Möbius transformations that is generated by the identifying transformations, which means Γ applied to $\mathscr{F}$ tesselates H^3 ($\Gamma(\mathscr{F})$ must completely cover H^3 without overlaps). If this is the case, the invariance of the Poincaré metric (1.1) under Γ guarantees that its restriction to $\mathscr{F}$ defines on the manifold $\mathscr{F}_M$ a smooth metric of constant sectional Gaussian curvature $-1/R^2$ (cf. [31]).

The identification pattern for the manifold $S \times]0,1[$, S a compact surface of genus two, is presented in fig. 1: We have drawn the base circles of ten hemispheres centered in the complex plane, the boundary of H^3. These hemispheres intersect just in the prescribed way. The domain $\mathscr{F}$ consists of the region exterior to all ten hemispheres in H^3 together with its bordering sides (geodesic planes) on the hemispheres. The manifold $\mathscr{F}_M \cong S \times]0,1[$ ($\cong$: homeomorphic) is just $\mathscr{F}$ with the side identification by the T_i, $i = 1,\ldots,5$. Every T_i (a lifted Möbius transformation) identifies two boundary planes by mapping the corresponding two hemispheres onto one another, so that (with the notation of fig. 1): $T_1(P_1) = P_4$, $T_1(P_2) = P_3$, $T_2(P_2) = P_5$, $T_2(P_3) = P_4$, $T_3(P_6) = P_9$, $T_3(P_7) = P_8$, $T_4(P_7) = P_{10}$, $T_4(P_8) = P_9$, $T_5(P_5) = P_1$, $T_5(P_6) = P_{10}$, and the same relations with P_i replaced by Q_i.

Let us for the moment attach the two bordering surfaces to $S \times]0,1[$, that makes it a compact manifold $S \times [0,1]$. In $H^3 \cup \mathbb{C} \cup \{\infty\}$ these two surfaces are presented (see fig. 1) by the interior f_1 and f_2 of two closed polygons with vertices P_i, $i = 1,\ldots,10$ and Q_i, $i = 1,\ldots,10$ (the second encloses the point at infinity), their circular arcs identified by the T_i. It is easy to imagine that this side identification gives rise to two compact surfaces of genus two. The other fibers of $S \times [0,1]$ can also easily be located in $\mathscr{F}$. For more pictorial details of the homeomorphism $\mathscr{F}_M \cong S \times]0,1[$ see Marden [29] and section 8.

Just as in our two-dimensional torus example we can realize geodesic motion on the hyperbolic manifold $\mathscr{F}_M$ by projecting geodesics in H^3 (semicircles orthogonal to the complex plane) into $\mathscr{F}_M$. The projection

map π is again defined so that if an image $\gamma(\mathscr{F})$, $\gamma \in \Gamma$ (the discrete group of Möbius transformations generated by the five identifying transformations T_i of $\mathscr{F}$), contains a piece of the geodesic in H^3, this piece is mapped by the inverse of γ into $\mathscr{F}$. (Technically: H^3 is the universal covering space of $\mathscr{F}_M$ and π is the natural projection of H^3 onto the quotient $H^3/\Gamma \cong \mathscr{F}_M$.)

To study further qualitatively geodesic motion on $\mathscr{F}_M$ we introduce the concept of limit points of the group Γ. From the construction of Γ it follows that it has countably many elements. Let us assume that it has infinitely many. If this is the case, the images of $\mathscr{F}$ under Γ tesselate the interior of the ten bordering hemispheres of $\mathscr{F}$ and therefore there are accumulation points of these images. These accumulation points cannot lie in H^3, for the geodesic boundary planes of $\gamma(\mathscr{F})$, $\gamma \in \Gamma$, enclose the same angles with one another like the corresponding planes of $\mathscr{F}$. These angles are non-zero, for the circles in fig. 1 do not touch but intersect each other, and so every polyhedron $\gamma(\mathscr{F})$ is surrounded by the same finite number of neighbouring polyhedra. Thus these limit points lie in the plane at infinity, in the discs defined by the base circles in fig. 1. Indeed, these limit points constitute a directed closed Jordan curve, in general of noninteger Hausdorff dimension: The limit set $\Lambda(\Gamma)$ of Γ (cf. sections 4–8).

Now consider the compact set $C(\Lambda)$ composed of all semicircles orthogonal to $\mathbb{C}$ with both initial and end point in the limit set. $C(\Lambda)$ is invariant under Γ for $\Lambda(\Gamma)$ is (cf. [26] or section 5). Its intersection with $\mathscr{F}$ is separated by a finite minimum distance from the plane at infinity. If an arbitrary semicircle of $C(\Lambda)$ is projected into $\mathscr{F}$, the arc-segments of this projection belong again to semicircles of $C(\Lambda)$ because of the invariance of $C(\Lambda)$: We obtain a bounded trajectory in $\mathscr{F}_M$, which is dense in $\mathscr{F} \cap C(\Lambda)$ or accidentally a closed loop.

Projections of H^3-geodesics whose initial or end points do not lie in $\Lambda(\Gamma)$ give rise to unbounded trajectories, that escape for $t \to +\infty$ or $t \to -\infty$ to the boundary of $\mathscr{F}_M$ which will, however, not be reached in a finite time. This is so because for $t \to +\infty$ or $t \to -\infty$ only finitely many polyhedra of the tesselation are met by the semicircle and in the last polyhedron the geodesic reaches the plane at infinity of H^3 (cf. (1.15), $y(t = \pm\infty) = 0$).

A trajectory with its end point in the limit set is recurrent in the following sense: For every x in $\mathscr{F}_M$ one can find a ball with center x which is met infinitely often by the track for $t \to +\infty$. This is so because if a ball around x is sufficiently large, infinitely many Γ-images of it are intersected by the semicircle (cf. [3, 7]). The same holds true for the initial point in the limit set and $t \to -\infty$. If the trajectory is dense in $\mathscr{F} \cap C(\Lambda)$ and x is in $\mathscr{F} \cap C(\Lambda)$ one can choose the ball around x arbitrarily small.

It follows that just these trajectories in H^3 which have both their end points and initial points in the limit set project to trajectories in $\mathscr{F}_M$ that are bounded and recurrent in both directions of time $t \to \pm\infty$. And conversely, every trajectory that is bounded and recurrent for $t \to -\infty$ and $t \to +\infty$ has, if lifted into H^3, both initial point and end point in the limit set $\Lambda(\Gamma)$. (To lift a trajectory $s_{\mathscr{F}}$ of $\mathscr{F}_M$ to H^3 means to find a geodesic s_{H^3} in H^3, so that $\pi(s_{H^3}) = s_{\mathscr{F}}$.)

2. The spectrum and the resolvent kernel of the Schrödinger operator on the hyperbolic manifold $\mathscr{F}_M$

Schrödinger's equation for geodesic motion on a curved three-dimensional Riemannian space with line element $ds^2 = \sum_{i,j=1}^{3} g_{ij}(x)\,dx_i\,dx_j$ reads

$$\frac{\hbar}{i}\frac{\partial\psi}{\partial t} = \frac{\hbar^2}{2m}\Delta\psi, \tag{2.1}$$

where Δ denotes the Laplace–Beltrami operator,

$$\Delta\psi = \sum_{i,j=1}^{3} \frac{1}{\sqrt{g}}\frac{\partial}{\partial x_i}\left(\sqrt{g}\,g^{ij}\frac{\partial\psi}{\partial x_j}\right). \tag{2.2}$$

Here (g^{ij}) is the inverse and g the determinant of the matrix (g_{ij}). (Sometimes a term proportional $\hbar^2/m \cdot \hat{R}(x)\psi$ is added on the right side of (2.1), cf. e.g. [21], stemming from a possible term $\sim \hat{R}(x)\psi(x)\psi(x)$ in the Lagrange functional for the field. $\hat{R}(x)$ denotes the curvature scalar which is for metric (1.1) a constant $\sim 1/R^2$. The modification of (0.1), an energy shift, is obvious.)

Via time separation $\psi = u \cdot \exp\{-i(E/\hbar)t\}$ one derives the eigenvalue equation for the energy operator,

$$-\frac{\hbar^2}{2m}\Delta u = Eu. \tag{2.3}$$

We will be concerned mainly with square-integrable solutions of (2.3),

$$\int_{\text{manifold}} \bar{u}u\sqrt{g}\,dx^3 < \infty,$$

$\sqrt{g}\,dx^3$ denotes the volume element of the Riemannian space.

In Poincaré's upper half-space model H^3 (2.3) reads (with (g_{ij}) as in (1.1))

$$-\frac{y_3^2}{R^2}\left(\frac{\partial^2}{\partial y_1^2}+\frac{\partial^2}{\partial y_2^2}+\frac{\partial^2}{\partial y_3^2}-\frac{1}{y_3}\frac{\partial}{\partial y_3}\right)u(y) = \lambda u(y), \tag{2.4}$$

with $y := (y_1, y_2, y_3)$ and

$$\lambda = 2mE/\hbar^2. \tag{2.5}$$

The eigenvalue problem (2.3) on the hyperbolic manifold $\mathscr{F}_M$ can be stated as follows (for notation and definitions see section 1): Find the solutions u of (2.4) in the fundamental domain $\mathscr{F}$ which satisfy the boundary conditions

$$u(T_i y) = u(y), \quad i = 1,\ldots,5, \tag{2.6}$$

on the geodesic boundary planes of $\mathscr{F}$ (which are identified in pairs by the generators T_i of Γ) and are square-integrable,

$$\int_{\mathscr{F}} u(y)\bar{u}(y)\frac{R^3}{y_3^3}\,dy^3 < \infty. \tag{2.7}$$

Completely equivalently stated: Find the solutions of (2.4) which are periodic in H^3 with respect to Γ,

$$u(\gamma y) = u(y), \quad \gamma \in \Gamma, \tag{2.8}$$

and square-integrable over $\mathscr{F}$. (Every function satisfying (2.6) in $\mathscr{F}$ can be extended to a function in H^3 satisfying (2.8), for $\mathscr{F}$ is a fundamental domain of the group Γ.)

For the actual analytic calculations of eigenvalues we use a more symmetrical model of hyperbolic space then H^3. View $H^3 := \{(y_1, y_2, y_3) \in \mathbb{R}^3, y_3 > 0\}$ imbedded in $\mathbb{R}^3$. By an inversion in the plane $y_3 = 0$ followed by an inversion in the sphere with center $R \cdot e_3 := (0, 0, R)$ and radius $\sqrt{2} \cdot R$ (cf. (1.5)), the upper

half-space is mapped onto the open ball $B^3 := \{x \in \mathbb{R}^3, |x|^2 < R^2\}$. This isometry Φ is explicitly given by ([3, 8])

$$\begin{aligned} &\Phi\colon H^3 \to B^3, \\ &\Phi\colon (y_1, y_2, y_3) \to \left(\frac{2y_1}{|y/R + e_3|^2}, \frac{2y_2}{|y/R + e_3|^2}, \frac{(|y/R|^2 - 1)R}{|y/R + e_3|^2} \right). \end{aligned} \tag{2.9}$$

The hyperbolic metric in H^3 (cf. (1.1)) is carried by this isometry into the metric

$$ds^2 = \frac{4(dx_1^2 + dx_2^2 + dx_3^2)}{\left(1 - \frac{|x|^2}{R^2}\right)^2} \tag{2.10}$$

in B^3.

Φ maps the boundary of H^3, i.e. the extended complex plane onto the sphere $|x|^2 = R^2$ (stereographic projection) and the point $R \cdot e_3$ in H^3 into the center of B^3. Φ is of course a conformal map, it leaves angles invariant. This ball model B^3 of hyperbolic geometry could have been obtained also from the standard model Q^3 (cf. (1.2), (1.3)) by stereographic projection in $\mathbb{R}^4$ from the top of the lower shell of the hyperboloid (1.2): The upper shell is projected onto the ball B^3, embedded into $\mathbb{R}^4$: $B^3 = \{x \in \mathbb{R}^4, x_0 = 0, x_1^2 + x_2^2 + x_3^2 < R^2\}$. The explicit formula for this isometry is given by (cf. [8])

$$\begin{aligned} &S\colon Q^3 \to B^3, \\ &S\colon (x_0, x_1, x_2, x_3) \to \left(0, \frac{x_1}{1 + x_0/R}, \frac{x_2}{1 + x_0/R}, \frac{x_3}{1 + x_0/R}\right). \end{aligned} \tag{2.11}$$

Combining the inverse of (2.9) and (2.11) we get the isometry between H^3 and Q^3 mentioned in section 1.

The action of the orientation-preserving invariance group of hyperbolic geometry $SL(2, \mathbb{C})/\{\pm 1\}$ (cf. section 1) on the ball model B^3 follows immediately from the corresponding action (1.7) on H^3 (lengths in (1.7) are measured in units of R) and the isometry Φ in (2.9):

$$\begin{aligned} &\gamma_{B^3}\colon B^3 \to B^3, \\ &\gamma_{B^3}\colon x \to \Phi \gamma_{H^3} \Phi^{-1}(x). \end{aligned} \tag{2.12}$$

(We denote the quantities in H^3 and B^3 with subscripts, if it is not clear from the context.) The inverse of Φ is given by

$$\begin{aligned} &\Phi^{-1}\colon B^3 \to H^3, \\ &\Phi^{-1}\colon (x_1, x_2, x_3) \to \left(\frac{2x_1}{|x/R - e_3|^2}, \frac{2x_2}{|x/R - e_3|^2}, \frac{(1 - |x/R|^2)R}{|x/R - e_3|^2} \right). \end{aligned} \tag{2.13}$$

B^3-Möbius transformations γ_{B^3} leave the line element (2.10) invariant and the geodesics in B^3 are arcs of circles orthogonal to the sphere at infinity $S_\infty := \{x \in \mathbb{R}^3, |x| = R\}$, the boundary of B^3. Hemispheres resting on the plane at infinity of H^3 are mapped by Φ into spheres orthogonal to S_∞ and the identification pattern of the base circles of these spheres on S_∞ remains that of fig. 1. The group

$\Gamma_{B^3} := \Phi\Gamma_{H^3}\Phi^{-1}$ of B^3-Möbius transformations is again conformal, preserves B^3 as well as S_∞, transforms spheres orthogonal to S_∞ onto spheres orthogonal to S_∞; $\mathscr{F}_{B^3} := \Phi(\mathscr{F}_{H^3})$ is a fundamental domain for Γ_{B^3} and the $\Phi T_i \Phi^{-1}$, $i = 1,\ldots,5$ are its side-identifying transformations, that give rise to a hyperbolic manifold $\mathscr{F}_{M,B^3}$, isometric via Φ to $\mathscr{F}_{M,H^3}$.

The analytic expression (2.12) for γ_{B^3} is rather involved, but there do exist simple formulae for the absolute value $|\gamma(x)|$ (we drop from now on the subscript B^3) and the Jacobi determinant $|\gamma'(x)|^3 := \det(\partial\gamma_i(x)/\partial x_j)$. Here $\gamma_i(x)$ denotes the ith component of the vector $\gamma(x)$, and $|\gamma'(x)|$ denotes the change of scale, which is the same in every direction (cf. Ahlfors [3]). For the derivation of the following formulae we refer to Ahlfors [3]:

$$|\gamma(x)| = \frac{|x-y|}{[x/R, y/R]} =: |T_y x|, \tag{2.14}$$

$$[x, y]^2 := 1 + |x|^2 \cdot |y|^2 - 2x \cdot y \tag{2.15}$$

and

$$y := \gamma^{-1}(0), \tag{2.16}$$

0 is of course the center of B^3. In terms of the $SL(2,\mathbb{C})$ matrix $\begin{pmatrix} a & b \\ c & d \end{pmatrix}$ which is represented by γ via (1.7) and (2.12) we calculate the components y_i of y as (note that $\Phi(R \cdot e_3) = 0$, cf. (2.9), (2.13))

$$\begin{aligned} y_1 &= \frac{2R \cdot \mathrm{Re}(-b\bar{a} - d\bar{c})}{|a|^2 + |b|^2 + |c|^2 + |d|^2 + 2}, \\ y_2 &= \frac{2R \cdot \mathrm{Im}(-b\bar{a} - d\bar{c})}{|a|^2 + |b|^2 + |c|^2 + |d|^2 + 2}, \\ y_3 &= \frac{R(|d|^2 + |b|^2 - |a|^2 - |c|^2)}{|a|^2 + |b|^2 + |c|^2 + |d|^2 + 2} \end{aligned} \tag{2.17}$$

and finally

$$|y|^2 = R^2 \frac{|a|^2 + |b|^2 + |c|^2 + |d|^2 - 2}{|a|^2 + |b|^2 + |c|^2 + |d|^2 + 2}. \tag{2.18}$$

(2.14) can also be written in the form

$$1 - |\gamma x|^2/R^2 = \frac{(1 - |x|^2/R^2)(1 - |y|^2/R^2)}{[x/R, y/R]^2}. \tag{2.19}$$

For the change of scale $|\gamma'(x)|$ and thus for the Jacobi determinant $|\gamma'(x)|^3$ Ahlfors [3] derives

$$|\gamma'(x)| = \frac{1 - |y/R|^2}{[x/R, y/R]^2} =: |T_y' x|. \tag{2.20}$$

Combining (2.19) and (2.20) we have another useful formula

$$\frac{|\gamma'(x)|}{1-\frac{1}{R^2}|\gamma(x)|^2}=\frac{1}{1-|x/R|^2}. \tag{2.21}$$

The special notation in (2.14) and (2.20) $|T_y x|$ and $|T_y' x|$ refers to the fact that both $|\gamma(x)|$ and $|\gamma'(x)|$ depend on the Möbius transformation γ only via $y=\gamma^{-1}(0)$ (cf. 2.17), and that the expressions (2.14) and (2.20) have (viewed as functions of x and y) interesting transformation properties under B^3-Möbius transformations β (cf. Ahlfors [3]):

$$|T_{\beta y}(\beta x)|=|T_y(x)|, \tag{2.22}$$

$$|T'_{\beta y}(\beta x)|\cdot|\beta'(x)|=|T_y'(x)|. \tag{2.23}$$

Moreover, the hyperbolic distance $d(x, y)$ with respect to the line element (2.10) between two points x, y in B^3 can be expressed by $|T_y x|$ (cf. Ahlfors [3] or Beardon [8]),

$$\cosh\frac{1}{R}d(x,y)=\frac{1+\frac{1}{R^2}|T_y x|^2}{1-\frac{1}{R^2}|T_y x|^2}. \tag{2.24}$$

The eigenvalue equation for the energy operator (2.3) in B^3 with metric (2.10) is given by

$$-\Delta_{B^3}u=\lambda u, \tag{2.25}$$

with λ as in (2.5) and Δ_{B^3} denotes the Laplace–Beltrami operator in B^3 (we use polar coordinates),

$$\Delta_{B^3}=\frac{\left(1-\frac{r^2}{R^2}\right)^2}{4}\left[\Delta_{E^3}+\frac{1}{R^2}\frac{2}{1-\frac{r^2}{R^2}}r\frac{\partial}{\partial r}\right]; \tag{2.26}$$

Δ_{E^3} is the Euclidean Laplace operator in polar coordinates,

$$\Delta_{E^3}u=\frac{1}{r}\frac{\partial^2(ru)}{\partial r^2}-\frac{1}{r^2}l^2u.$$

The operator l^2 contains the angular dependence of Δ_{E^3}. It is well known, that the surface spherical harmonics (cf. e.g. [27]) $Y_l^m(\vartheta,\varphi)$, $l=1,\ldots,\infty$; $m=-l,\ldots,l$, are eigenfunctions of l^2,

$$l^2Y_l^m(\vartheta,\varphi)=l(l+1)Y_l^m(\vartheta,\varphi),$$

and provide a complete orthonormal system on the unit sphere.

For future reference we list

$$Y_0^0(\vartheta,\varphi)=\frac{1}{\sqrt{4\pi}}, \tag{2.27}$$

$$\int_0^{2\pi}\int_0^{\pi} Y_l^m(\vartheta,\varphi)\sin\vartheta\,\mathrm{d}\vartheta\,\mathrm{d}\varphi=0 \quad \text{if } l\neq 0. \tag{2.28}$$

Thus, if we make the ansatz $u=\mathscr{R}(r)\cdot Y_l^m(\vartheta,\varphi)$ in (2.25) we get the eigenvalue equation for the radial dependence $\mathscr{R}(r)$ of u,

$$-\frac{\left(1-\frac{r^2}{R^2}\right)^2}{4}\left[\frac{\mathrm{d}^2\mathscr{R}(r)}{\mathrm{d}r^2}+2\frac{\mathrm{d}\mathscr{R}(r)}{\mathrm{d}r}-\frac{l(l+1)}{r^2}\mathscr{R}(r)+\frac{1}{R^2}\frac{2}{1-\frac{r^2}{R^2}}r\frac{\mathrm{d}\mathscr{R}(r)}{\mathrm{d}r}\right]=\lambda\mathscr{R}(r). \tag{2.29}$$

Changing variables in (2.29) (cf. [15]),

$$\sigma=\frac{1}{1-\frac{r^2}{R^2}},$$

we arrive at a generalized hypergeometric differential equation (cf. [27]), $\hat{\mathscr{R}}(\sigma):=\mathscr{R}(R\sqrt{(\sigma-1)/\sigma})$,

$$\frac{\mathrm{d}^2\hat{\mathscr{R}}(\sigma)}{\mathrm{d}^2\sigma}+\frac{3}{2}\left(\frac{1}{\sigma}+\frac{1}{\sigma-1}\right)\frac{\mathrm{d}\hat{\mathscr{R}}(\sigma)}{\mathrm{d}\sigma}+\frac{1}{\sigma(\sigma-1)}\left(\frac{-l(l+1)}{4(\sigma-1)\sigma}+R^2\lambda\right)\hat{\mathscr{R}}(\sigma)=0. \tag{2.30}$$

There is only one linearly independent solution of (2.30) that is finite at $\sigma=1$ (which is provided by function W_{11} in [27] on p. 61). From this we conclude that the only linearly independent solution of (2.29) that stays finite at $r=0$ is given by (we write from now on $\mathscr{R}_{\lambda,l}(r)$ for $\mathscr{R}(r)$)

$$\mathscr{R}_{\lambda,l}(r)=\left(\frac{r}{R}\right)^{2\left(-\frac{1}{4}+\frac{1}{2}\sqrt{1/4+l(l+1)}\right)}\left(1-\left(\frac{r}{R}\right)^2\right)^{1-\sqrt{1-\lambda R^2}}$$
$$\cdot{}_2F_1\left(\tfrac{1}{2}+\sqrt{1/4+l(l+1)}-\sqrt{1-\lambda R^2},\tfrac{1}{2}-\sqrt{1-\lambda R^2},1+\sqrt{1/4+l(l+1)},\left(\frac{r}{R}\right)^2\right) \tag{2.31}$$

($\sqrt{1-\lambda R^2}$ denotes the principal value: $\pi/2\geq\arg(\sqrt{1-\lambda R^2})>-\pi/2$).

For $r\to R$ and $\mathrm{Re}(\sqrt{1-\lambda R^2})>0$, $\mathscr{R}_{\lambda,l}(r)$ behaves asymptotically as

$$\mathscr{R}_{\lambda,l}(r)\sim\text{const.}\left(1-\left(\frac{r}{R}\right)^2\right)^{1-\sqrt{1-\lambda R^2}}. \tag{2.32}$$

Thus the solutions of (2.29) for real λ that stay finite on the sphere at infinity S_∞ of B^3 are those with $\lambda R^2\geq 0$.

Every eigenfunction of $-\Delta_{B^3}$ admits a convergent "Fourier" expansion of the form (cf. [15])

$$u_\lambda(r,\vartheta,\varphi)=\sum_{l=0}^{\infty}\sum_{m=-l}^{+l}a_{ml}\mathscr{R}_{\lambda,l}(r)Y_l^m(\vartheta,\varphi) \tag{2.33}$$

and the eigenfunction that is independent of ϑ and φ is provided up to a multiplicative constant by (cf. [27], p. 39)

$$u_\lambda(r)=\mathscr{R}_{\lambda,0}(r)=\left(1-\left(\frac{r}{R}\right)^2\right)^{1-\sqrt{1-\lambda R^2}}\frac{R}{4r\sqrt{1-\lambda R^2}}\left[\left(1+\frac{r}{R}\right)^{2\sqrt{1-\lambda R^2}}-\left(1-\frac{r}{R}\right)^{2\sqrt{1-\lambda R^2}}\right]. \tag{2.34}$$

To construct the resolvent kernel of the operator $-\Delta_{B^3}$ (i.e. the Green function for the operator $-(\Delta_{B^3}+\lambda)$) we proceed as follows (cf. Ahlfors [3]): At first we define (up to a multiplicative constant) the Green function with pole at $r=0$ as the angle-independent solution of (2.25) that is singular at $r=0$ and decays as fast as possible for $r\to R$. A solution of (2.29) for $l=0$ that provides a pole at $r=0$ and is bounded for $r\to R$ is again given by (2.31) if one replaces the root $\sqrt{1/4+l(l+1)}$ by $-\sqrt{1/4+l(l+1)}$. (This corresponds to solution W_{12} of (2.30) in [27] on p. 61). Thus an angle-independent solution $g_\lambda(r)$ of (2.25) is

$$g_\lambda(r)=\left(\frac{r}{R}\right)^{-1}\left(1-\left(\frac{r}{R}\right)^2\right)^{1-\sqrt{1-\lambda R^2}}\frac{1}{2}\left[\left(1+\frac{r}{R}\right)^{2\sqrt{1-\lambda R^2}}+\left(1-\frac{r}{R}\right)^{2\sqrt{1-\lambda R^2}}\right] \tag{2.35}$$

and the Green function with pole at $\boldsymbol{0}$ is therefore

$$G_\lambda(r)=c_1(g_\lambda(r)+c_2\mathscr{R}_{\lambda,0}(r)), \tag{2.36}$$

with $c_2=-2\sqrt{1-\lambda R^2}$ determined by the decay condition and $c_1=(8\pi R)^{-1}$ (see below).

We have for $r\to 0$

$$G_\lambda(r)=\frac{1}{8\pi}\frac{1}{r}+\mathcal{O}(1) \tag{2.37}$$

and for $r\to R$

$$G_\lambda(r)\sim\text{const.}\left(1-\left(\frac{r}{R}\right)^2\right)^{1+\sqrt{1-\lambda R^2}}. \tag{2.38}$$

To obtain the Green function with pole at y, $y\in B^3$, we use the fact that Δ_{B^3} is invariant under B^3-Möbius transformations γ, because Δ_{B^3} is the Laplace–Beltrami operator of the invariant (cf. (2.21)) metric (2.10). Therefore, if $G_\lambda(|x|)$ solves (2.25) the same is true for (cf. Ahlfors [3])

$$G_\lambda(|\gamma x|)=G_\lambda(|T_y x|)=:G_\lambda(x,y). \tag{2.39}$$

$G_\lambda(x,y)$ is the Green function with pole at y (cf. (2.14), (2.15) for the definition of $|T_y x|$; see also [16] for the corresponding expression of $G_\lambda(x,y)$ in H^3).

By definition $G_\lambda(x, y)$ is the inverting kernel of $-(\Delta_{B^3}+\lambda)$ and we have

$$v(x)=\int_{B^3} G_\lambda(x, y)[-\Delta_{B^3}-\lambda]v(y)\,\mathrm{d}y_\mathrm{h} \tag{2.40}$$

for every $v(x)$ that is sufficiently smooth, say in $C^2(B^3)$, and decays sufficiently fast for $|\boldsymbol{x}|\to R$ so that the integral makes sense. $\mathrm{d}y_\mathrm{h}$ denotes the hyperbolic volume element with respect to the metric (2.10),

$$\mathrm{d}y_\mathrm{h}=\frac{8\mathrm{d}^3y}{\left(1-|y/R|^2\right)^3}. \tag{2.41}$$

The constant c_1 in (2.36) can be determined by a special choice of v in (2.40). Note, however, that the Euclidean Green function has a pole of the form $(1/4\pi)(1/r)$. Thus the pole (2.37) of $G_\lambda(x, y)$ is strongly suggested by the form of the Laplace–Beltrami operator (2.26) and the volume element (2.41) for $r=|y|\to 0$.

We obtain the Green function of the manifold $\mathscr{F}_\mathrm{M}$ by restricting the $\Gamma\times\Gamma$-periodic function

$$G_\lambda^\Gamma(x, y)=\sum_{\gamma\in\Gamma} G_\lambda(x, \gamma y) \tag{2.42}$$

in $B^3\times B^3$ to $\mathscr{F}\times\mathscr{F}$ (cf. Ahlfors [3]; compare also (2.6) and (2.8)). By definition G_λ^Γ satisfies (2.25) in both variables and from the properties of the fundamental domain $\mathscr{F}$ ($y\in\mathscr{F}\Rightarrow\gamma(y)\notin\mathscr{F}$ if $\gamma\neq\mathrm{id}$) it follows that for $x\to y$

$$G_\lambda^\Gamma(x, y)=\frac{1}{8\pi}\frac{1}{|x-y|}+\mathcal{O}(1). \tag{2.43}$$

$G_\lambda^\Gamma(x, y)$ is symmetric in x and y, for $G_\lambda(x, y)$ is ($|T_y x|=|T_x y|$ in (2.39)) and from (2.22) it follows that G_λ^Γ is $\Gamma\times\Gamma$ periodic. For $\gamma_1, \gamma_2\in\Gamma$ we get

$$G_\lambda^\Gamma(\gamma_1 x, \gamma_2 y)=G_\lambda^\Gamma(x, y). \tag{2.44}$$

Analogous to (2.40) for all v in $C^2(\mathscr{F}_\mathrm{M})$ and $L^2(\mathscr{F}_\mathrm{M}, \mathrm{d}y_\mathrm{h})$ we have

$$v(x)=\int_{\mathscr{F}_\mathrm{M}} G_\lambda^\Gamma(x, y)\left[-\Delta_{\mathscr{F}_\mathrm{M}}-\lambda\right]v(y)\,\mathrm{d}y_\mathrm{h}, \tag{2.45}$$

where $\Delta_{\mathscr{F}_\mathrm{M}}$ is the Laplace–Beltrami operator on $\mathscr{F}_\mathrm{M}$ obtained by restricting Δ_{B^3} to $\mathscr{F}$. $C^2(\mathscr{F}_\mathrm{M})$ and $L^2(\mathscr{F}_\mathrm{M}, \mathrm{d}y_\mathrm{h})$ means sufficiently smooth, periodic with respect to Γ, and square-integrable on $\mathscr{F}$ via the volume element (2.41); compare (2.6), (2.7), (2.8). $G_\lambda^\Gamma(x, y)$, being the kernel of $[-\Delta_{\mathscr{F}_\mathrm{M}}-\lambda]^{-1}$ in $L^2(\mathscr{F}_\mathrm{M}, \mathrm{d}y_\mathrm{h})$, will not exist for values of λ at which the inverse of $-\Delta_{\mathscr{F}_\mathrm{M}}-\lambda$ does not exist. Therefore we expect that the series (2.42) and its analytic continuation will develop singularities for these real λ which correspond to square-integrable eigenfunctions of $-\Delta_{\mathscr{F}_\mathrm{M}}$. This is just the strategy to locate the ground state.

At first we replace the series (2.42) by an analytically simpler one, that has the same convergence properties as $G_\lambda^\Gamma(x, y)$. We put $x=\boldsymbol{0}$ in (2.42) and fix $y\in\mathscr{F}$. Then the sequence $(|\gamma y|)$, $\gamma\in\Gamma$, converges

to R, the radius of B^3, because there are only finitely many images of the fundamental domain $\mathscr{F}$ in a ball centered at the origin with radius $R-\varepsilon$, $\varepsilon>0$. Thus only finitely many $|\gamma y|$ are smaller than $R-\varepsilon$ for every $\varepsilon>0$. Therefore we can replace $G_\lambda(\boldsymbol{0},\gamma y)$ in (2.42) by its asymptotic expression (2.38) and end up with a series (cf. Ahlfors [3])

$$H(y,\lambda):=\sum_{\gamma\in\Gamma}\left(1-\frac{|\gamma y|^2}{R^2}\right)^{1+\sqrt{1-\lambda R^2}}. \tag{2.46}$$

(We take the principal value of the root, as defined in (2.31).)

Next we show, that if

$$h(y,s):=\sum_{\gamma\in\Gamma}\left(1-\left|\frac{\gamma y}{R}\right|^2\right)^{1+s} \tag{2.47}$$

converges for $y=\boldsymbol{0}$, then there exist two positive constants c_1, c_2, so that [34]

$$c_2\left(1-\left|\frac{y}{R}\right|^2\right)^{1+s}\sum_{\gamma\in\Gamma}\left(1-\left|\frac{\gamma\boldsymbol{0}}{R}\right|^2\right)^{1+s}<h(y,s)<c_1\left(1-\left|\frac{y}{R}\right|^2\right)^{1+s}\sum_{\gamma\in\Gamma}\left(1-\left|\frac{\gamma\boldsymbol{0}}{R}\right|^2\right)^{1+s} \tag{2.48}$$

uniformly (i.e. c_1, c_2 are independent of y) for all y in a given fundamental domain $\mathscr{F}$. In the following convergence considerations we put $R=1$. Applying (2.14), (2.19)–(2.21) we have (cf. Patterson [34])

$$\begin{aligned}h(y,s)&=\sum_{\gamma\in\Gamma}\left(1-|T_{\gamma\boldsymbol{0}}y|^2\right)^{1+s}=\left(1-|y|^2\right)^{1+s}\sum_{\gamma\in\Gamma}|T'_{\gamma\boldsymbol{0}}y|^{1+s}\\&=\left(1-|y|^2\right)^{1+s}\sum_{\gamma\in\Gamma}\frac{\left(1-|\gamma\boldsymbol{0}|^2\right)^{1+s}}{[y,\gamma\boldsymbol{0}]^{2(1+s)}}.\end{aligned}$$

It follows from the definition (2.15) of $[x,y]^2$ that $[x,y]^2\le 4$. On the other hand $[y,\gamma\boldsymbol{0}]>|y-\gamma\boldsymbol{0}|>c>0$ uniformly for all $y\in\mathscr{F}$ and all $\gamma\in\Gamma$, $\gamma\boldsymbol{0}\notin\mathscr{F}$. This is so because $\mathscr{F}$ and the limit set $\Lambda(\Gamma)$, defined as the set of accumulation points of images of $\mathscr{F}$ (cf. section 1) or equivalently as the set of accumulation points of the sequence $(\gamma\boldsymbol{0})$, $\gamma\in\Gamma$ (cf. [26]), are separated by a finite minimum distance.

By similar reasoning one proves that the series $h(y,s)$ converges for $\mathrm{Re}(s)>1$ (Ahlfors [3]): Denoting by $\mathrm{d}y_{\mathrm{h}}(x)$ the volume element (2.41) invariant under Γ ($\mathrm{d}y_{\mathrm{h}}(\gamma x)=\mathrm{d}y_{\mathrm{h}}(x)$, $\gamma\in\Gamma$), we have for $\mathrm{Re}(s)>1$ ($R=1$)

$$\begin{aligned}\infty>\int_{B^3}\left(1-|x|^2\right)^{1+s}\mathrm{d}y_{\mathrm{h}}(x)&=\sum_{\gamma\in\Gamma}\int_{\gamma(\mathscr{F})}\left(1-|x|^2\right)^{1+s}\mathrm{d}y_{\mathrm{h}}(x)\\&=\sum_{\gamma\in\Gamma}\int_{\mathscr{F}}\left(1-|\gamma x|^2\right)^{1+s}\mathrm{d}y_{\mathrm{h}}(x)>\text{const.}\sum_{\gamma\in\Gamma}\int_{\mathscr{F}}\left(1-|\gamma\boldsymbol{0}|^2\right)^{1+s}\left(1-|x|^2\right)^{1+s}\mathrm{d}y_{\mathrm{h}}(x).\end{aligned}$$

Actually one can show (Ahlfors [3]) that the series $h(y,s)$ is convergent even for $\mathrm{Re}(s)=1$ if the fundamental polyhedron $\mathscr{F}$ has sides lying on the sphere at infinity S_∞ of B^3 (f_1 and f_2 in fig. 1).

Turning back to $H(y,\lambda)$ in (2.46) we know now that this series converges for $\lambda R^2 < 0$, and so the square-integrable eigenfunctions of $-\Delta_{\mathscr{F}_M}$ (cf. (2.45)) must have eigenvalues $\lambda \geq 0$. We will see later that the ground state λ_0 in our examples satisfies $1 > \lambda_0 R^2 > 0$ and therefore determines (and is determined by) the convergence abscissa of the series $H(y,\lambda)$ or $G^\Gamma_\lambda(x,y)$.

If λ_0 lies in the interval $]0, 1/R^2[$ (what we will from now on assume), then $G^\Gamma_\lambda(x,y)$ has the following analytic properties (cf. Elstrodt et al. [16], Patterson [33]): Writing $\lambda = (1-s^2)/R^2$, the function $G^\Gamma_\lambda(x,y)$ given by the series (2.42) for $\mathrm{Re}(s) > s_0 = \sqrt{1-\lambda_0 R^2}$ can be meromorphically continued into the whole half-plane $\mathrm{Re}(s) > 0$. It has there a possibly infinite number of poles s_i, $i = 1, \ldots, N$, all of them lying on the real axis in the interval $]0, s_0]$ (s_0 is one of them). If $N = \infty$ then the sequence (s_i) converges to 0. The corresponding λ_i, $i = 1, \ldots, N$ in $[\lambda_0, 1/R^2[$ are eigenvalues of the square-integrable eigenfunctions of $-\Delta_{\mathscr{F}_M}$ and separated from the continuous spectrum of $-\Delta_{\mathscr{F}_M}$, which is contained in $[1/R^2, \infty[$, where the root in (2.46) gets purely imaginary. The L^2-eigenfunctions and the generalized eigenfunctions of the continuous spectrum constitute of course a complete orthonormal system in $L^2(\mathscr{F}_M, \mathrm{d}y_h)$, for $-\Delta_{\mathscr{F}_M}$ is self-adjoined.

3. The construction of the ground state eigenfunction

In this section we employ Selberg's theory of point-pair invariants, which is the crucial tool in setting up the trace formula, to derive an explicit expression for the ground state eigenfunction (cf. Patterson [34]).

A point-pair invariant $K(x,y)$ is a function K: $B^3 \times B^3 \to \mathbb{C}$ that has the following invariance property under B^3-Möbius transformations γ:

$$K(\gamma x, \gamma y) = K(x,y). \tag{3.1}$$

We will be concerned with invariants of the form

$$K(x,y) = k(|T_y x|), \tag{3.2}$$

where k is a reasonably smooth function $\mathbb{R}^+ \to \mathbb{R}$. For the definition and invariance properties of $|T_y x|$ we refer to (2.14), (2.15), (2.22).

Let $u_\lambda(y)$ be an eigenfunction of $-\Delta_{B^3}$ (cf. (2.25), (2.33)) and $K(x,y)$ a point-pair invariant (3.2), so that the following integral exists. Then we have, with $\mathrm{d}y_h$ as in (2.41),

$$\int_{B^3} K(x,y)\overline{u_\lambda(y)}\,\mathrm{d}y_h = \Lambda_k(\lambda)\overline{u_\lambda(x)} \tag{3.3}$$

and $\Lambda_k(\lambda)$ does not depend on the eigenfunction u_λ, i.e. not on the coefficients a_{ml} in (2.33), but only on the eigenvalue λ and the function k in (3.2). At first we prove (3.3) for $x = \mathbf{0}$ (cf. [16, 22]):

Introducing polar coordinates, the integral in (3.3) reads

$$\int_0^R \int_0^{2\pi} \int_0^{\pi} k(r)\overline{u_\lambda(r,\vartheta,\varphi)}\,\frac{8r^2}{\left(1-\frac{r^2}{R^2}\right)^3}\sin\vartheta\,\mathrm{d}\vartheta\,\mathrm{d}\varphi\,\mathrm{d}r.$$

Inserting (2.33) for u_λ and performing the angular integration by means of (2.27), (2.28) gives

$$\Lambda_k(\lambda)\overline{u_\lambda(\boldsymbol{0})} = \overline{a_{00}} 16\pi^{1/2} \int_0^R k(r) \mathscr{R}_{\lambda,0}(r) \frac{r^2}{\left(1-\frac{r^2}{R^2}\right)^3} \mathrm{d}r.$$

On the other hand, from (2.31) and (2.33) we get

$$u_\lambda(\boldsymbol{0}) = \frac{1}{2\pi^{1/2}} a_{00}$$

and for $\Lambda_k(\lambda)$ we have therefore, independent of u_λ,

$$\Lambda_k(\lambda) = 32\pi \int_0^R k(r) \mathscr{R}_{\lambda,0}(r) \frac{r^2}{\left(1-\frac{r^2}{R^2}\right)^3} \mathrm{d}r. \tag{3.4}$$

To prove formula (3.3) for general x, choose a B^3-Möbius transformation γ so that $\gamma\boldsymbol{0} = x$. Then apply the invariance of $\mathrm{d}y_\mathrm{h}$ and $K(x, y)$ under Möbius transformations, and the fact that $u_\lambda(\gamma x)$ is also an eigenfunction to the eigenvalue λ because of the invariance of Δ_{B^3} under γ.

Let $u_\lambda^\Gamma(x)$ be an eigenfunction of $-\Delta_{B^3}$ that is periodic with respect to Γ,

$$u_\lambda^\Gamma(\gamma x) = u_\lambda^\Gamma(x), \quad \gamma \in \Gamma.$$

Then we have from (3.3) and the invariance of $\mathrm{d}y_\mathrm{h}$, $K(x, y)$ and $u_\lambda^\Gamma(x)$ under Γ

$$\begin{aligned} \int_{B^3} K(x, y)\overline{u_\lambda^\Gamma(y)}\,\mathrm{d}y_\mathrm{h} &= \sum_{\gamma\in\Gamma} \int_{\gamma(\mathscr{F})} K(x, y)\overline{u_\lambda^\Gamma(y)}\,\mathrm{d}y_\mathrm{h} \\ &= \int_{\mathscr{F}} \sum_{\gamma\in\Gamma} K(x, \gamma y)\overline{u_\lambda^\Gamma(y)}\,\mathrm{d}y_\mathrm{h} = \Lambda_k(\lambda)\overline{u_\lambda^\Gamma(x)}. \end{aligned} \tag{3.5}$$

$\mathscr{F}$ denotes of course a fundamental domain of Γ.

It follows from the definition of point-pair invariants (3.1), that the function

$$K^\Gamma(x, y) := \sum_{\gamma\in\Gamma} K(x, \gamma y) \tag{3.6}$$

is $\Gamma\times\Gamma$ periodic: For $\gamma_1, \gamma_2 \in \Gamma$

$$K^\Gamma(\gamma_1 x, \gamma_2 y) = K^\Gamma(x, y).$$

Let us choose k in (3.2) so that $K^\Gamma(x, y)$ is square-integrable in $\mathscr{F}$. For every $y \in \mathscr{F}$ we assume

$$\int_{\mathscr{F}} K^\Gamma(x, y)\overline{K^\Gamma(x, y)}\,\mathrm{d}y_\mathrm{h}(x) < \infty. \tag{3.7}$$

Then K^Γ admits an expansion in $L^2(\mathscr{F}_M, \mathrm{d}y_h)$ eigenfunctions $\varphi_{\lambda_n,j}(x)$ and generalized non-square-integrable eigenfunctions $E(\lambda,\vartheta,\varphi,x)$ of $-\Delta_{\mathscr{F}_M}$. ϑ, φ and j are degeneration indices and $E(\lambda,\vartheta,\varphi,x)$ satisfies

$$(\Delta_{\mathscr{F}_M}+\lambda)E(\lambda,\vartheta,\varphi,x)=0, \tag{3.8}$$

with $\lambda > 1/R^2$ (continuous spectrum, cf. the end of section 2).

$$K^\Gamma(x,y)=\sum_{n=0}^{N}\sum_{j=1}^{M_n} c_{n,j}\overline{\varphi_{\lambda_n,j}(x)}\,\varphi_{\lambda_n,j}(y) + \int_{1/R^2}^{\infty}\mathrm{d}\mu(\lambda)\int_{f_1\cup f_2}\sin\vartheta\,\mathrm{d}\vartheta\,\mathrm{d}\varphi\, c(\lambda,\vartheta,\varphi)\overline{E(\lambda,\vartheta,\varphi,x)}E(\lambda,\vartheta,\varphi,y), \tag{3.9}$$

here $\mu(\lambda)$ denotes spectral measure, M_n multiplicity and f_1, f_2 the two boundary domains of the fundamental polyhedron $\mathscr{F}$ on the sphere at infinity S_∞ of B^3 (see fig. 1). (For explicit expressions for the Eisenstein series $E(\lambda,\vartheta,\varphi,x)$ on manifolds with infinite hyperbolic volume see Patterson [33, 35].)

Inserting (3.9) into the last equation in (3.5) we get for the Fourier coefficients $c_{n,j}$ and $c(\lambda,\vartheta,\varphi)$

$$\begin{aligned} c_{n,j} &= \Lambda_k(\lambda_n),\\ c(\lambda,\vartheta,\varphi) &= \Lambda_k(\lambda), \end{aligned} \tag{3.10}$$

where $\Lambda_k(\lambda)$ is determined by (3.4). Now we specify the point-pair invariant $K(x,y)$, i.e. the function k in (3.2) in such a way, that $K^\Gamma x, y)$ becomes for $x=\boldsymbol{0}$ the Poincaré series $h(y,s)$ in (2.47). The following choice does it:

$$k(|T_x y|)=\left(1-\frac{1}{R^2}|T_x y|^2\right)^{1+s}. \tag{3.11}$$

With this k we evaluate the integral in (3.4) and obtain (cf. [27], p. 55)

$$\begin{aligned} \Lambda_k(\lambda) &= 32\pi\int_0^R \mathrm{d}r\, r^2\left(1-\frac{r^2}{R^2}\right)^{-1+s-\sqrt{1-\lambda R^2}}\,{}_2F_1\left(1-\sqrt{1-\lambda R^2},\tfrac{1}{2}-\sqrt{1-\lambda R^2},\tfrac{3}{2},\left(\frac{r}{R}\right)^2\right)\\ &= 8\pi^{3/2}R^3\frac{\Gamma(s-\sqrt{1-\lambda R^2})\Gamma(s+\sqrt{1-\lambda R^2})}{\Gamma(\frac{1}{2}+s)\Gamma(1+s)} =: \Lambda(s,\lambda) \end{aligned} \tag{3.12}$$

and for the Poincaré series $K^\Gamma(\boldsymbol{0},y)$ with k as in (3.11)) we get (cf. (3.6), (3.9))

$$\begin{aligned} h(s,y)=K^\Gamma(\boldsymbol{0},y) &= \sum_{\gamma\in\Gamma}\left(1-\frac{|\gamma y|^2}{R^2}\right)^{1+s}\\ &= \sum_{n=0}^{N}\sum_{j=1}^{M_n}\Lambda(s,\lambda_n)\overline{\varphi_{\lambda_n,j}(\boldsymbol{0})}\,\varphi_{\lambda_n,j}(y)\\ &\quad + \int_{1/R^2}^{\infty}\mathrm{d}\mu(\lambda)\,\Lambda(s,\lambda)\int_{f_1\cup f_2}\sin\vartheta\,\mathrm{d}\vartheta\,\mathrm{d}\varphi\,\overline{E(\lambda,\vartheta,\varphi,\boldsymbol{0})}\,E(\lambda,\vartheta,\varphi,y). \end{aligned} \tag{3.13}$$

Assume as in section 2, that the ground state λ_0 lies in $]0, 1/R^2[$. Then we see immediately from (3.12) that $\Lambda(s, \lambda_0)$ has a simple pole for $s = \sqrt{1 - \lambda_0 R^2} =: s_0$, and from (3.13) it follows that $h(y, s)$ has a simple pole at $s = s_0$ too, which is the convergence abscissa of $h(y, s)$ (cf. section 2). Moreover we have from (3.13) that

$$\varphi_{\text{g.st.}}(y) := \lim_{s \to s_0} (s - s_0) \cdot h(y, s) = \text{const} \cdot \sum_{j=1}^{M_0} \overline{\varphi_{\lambda_0, j}(\boldsymbol{0})}\, \varphi_{\lambda_0, j}(y) \tag{3.14}$$

is an eigenfunction of $-\Delta_{\mathcal{F}_M}$ to the ground state eigenvalue λ_0. One can show (cf. Patterson [34], Sullivan [41–43]) that the eigenspace of λ_0 is one-dimensional ($M_0 = 1$ in (3.14)): $\varphi_{\text{g.st.}}(y)$ is the unique ground state. The square-integrability of $\varphi_{\text{g.st.}}(y)$ and of $K^{\Gamma}(x, y)$ (cf. (3.7)) with k as in (3.11) follows from (2.48).

The ground state energy E_0 and the abscissa of convergence s_0 of $h(y, s)$ (cf. (3.13) or (2.47)) are therefore connected by (cf. (2.5))

$$s_0 = \sqrt{1 - 2mE_0R^2/\hbar^2} \tag{3.15}$$

provided $s_0 > 0$. From the convergence considerations for the series $h(y, s)$ in section 2 we know already that $s_0 < 1$. Our previous assumption $0 < \lambda_0 R^2 < 1$ corresponds to $1 > s_0 > 0$ (see the end of section 2).

In the next section we will connect s_0 with the Hausdorff dimension of the limit set $\Lambda(\Gamma)$ of the group Γ, thus establishing the relation mentioned in the introduction.

4. The Poincaré series $h(y, s)$ as a supplier of Hausdorff covers for the limit set $\Lambda(\Gamma)$ and the connection between Hausdorff dimension of $\Lambda(\Gamma)$ and convergence abscissa of $h(y, s)$

We work in this section again with the B^3-model of hyperbolic space. The hyperbolic distance $d(\boldsymbol{0}, \boldsymbol{x})$ in B^3 between the center $\boldsymbol{0}$ and a point $\boldsymbol{x}$ that has Euclidean distance $r = |\boldsymbol{x}|$ from $\boldsymbol{0}$ is easily calculated from the geodesic line element in (2.10) and given by

$$d(\boldsymbol{0}, \boldsymbol{x}) = R \log \frac{1 + \frac{r}{R}}{1 - \frac{r}{R}}. \tag{4.1}$$

Denoting by $d(\boldsymbol{x}, \boldsymbol{y})$ hyperbolic distance between two points $\boldsymbol{x}, \boldsymbol{y}$ (cf. (2.24)), a hyperbolic sphere $S(\boldsymbol{a}_{\text{H}}, \rho_{\text{H}})$ with hyperbolic center $\boldsymbol{a}_{\text{H}}$ and radius ρ_{H} is defined by

$$S(\boldsymbol{a}_{\text{H}}, \rho_{\text{H}}) := \{\boldsymbol{x} | d(\boldsymbol{a}_{\text{H}}, \boldsymbol{x}) = \rho_{\text{H}}\}.$$

If we transform $\boldsymbol{a}_{\text{H}}$ into the center of B^3 by a B^3-Möbius transformation (cf. section 2), we see because of the invariance of $d(\boldsymbol{x}, \boldsymbol{y})$ under Möbius transformations and their property that spheres are transformed into spheres (cf. sections 1 and 2) that $S(\boldsymbol{a}_{\text{H}}, \rho_{\text{H}})$ is also a sphere in the Euclidean sense.

The Euclidean radius r_E of $S(\boldsymbol{a}_H, \rho_H)$ is calculated via (4.1) (and the inverse of it) as (cf. Ahlfors [3])

$$r_E = \tfrac{1}{2}\left[R\tanh\tfrac{1}{2}\left(\log\frac{1+\frac{|\boldsymbol{a}_H|}{R}}{1-\frac{|\boldsymbol{a}_H|}{R}} + \frac{\rho_H}{R}\right) - R\tanh\tfrac{1}{2}\left(\log\frac{1+\frac{|\boldsymbol{a}_H|}{R}}{1-\frac{|\boldsymbol{a}_H|}{R}} - \frac{\rho_H}{R}\right)\right]$$

$$= R\frac{\left(1-\frac{|\boldsymbol{a}_H|^2}{R^2}\right)\tanh\frac{\rho_H}{2R}}{1-\frac{|\boldsymbol{a}_H|^2}{R^2}\tanh^2\frac{\rho_H}{2R}}$$

and similarly the Euclidean center $\boldsymbol{m}_E := (\boldsymbol{a}_H/|\boldsymbol{a}_H|)|\boldsymbol{m}_E|$ with

$$|\boldsymbol{m}_E| = \frac{|\boldsymbol{a}_H|\left(1-\tanh^2\frac{\rho_H}{2R}\right)}{1-\frac{|\boldsymbol{a}_H|^2}{R^2}\tanh^2\frac{\rho_H}{2R}}.$$

For $x := e^{\rho_H/R}(1-|\boldsymbol{a}_H|^2/R^2) \ll 1$ we have

$$\begin{aligned} |r_E| &= R\left[c_r(\rho_H/R)x + \mathcal{O}(x^2)\right], \\ |m_E| &= R\left[1 - c_M(\rho_H/R)x + \mathcal{O}(x^2)\right] \end{aligned} \tag{4.2}$$

where the coefficient functions c_r and c_M admit for $\rho_H/R \ll 1$ expansions in ρ_H/R and for $\rho_H/R \gg 1$ expansions in $e^{-\rho_H/R}$. (4.2) tells us (cf. Ahlfors [3]) that if a hyperbolic ball $B(\boldsymbol{a}_H, \rho_H) := \{\boldsymbol{x} | d(\boldsymbol{a}_H, \boldsymbol{x}) \leq \rho_H\}$ is sufficiently close to the boundary S_∞ of B^3, its Euclidean radius and the distance between its Euclidean center and the sphere at infinity S_∞ are both proportional to $1-|\boldsymbol{a}_H|^2/R^2$.

Now let $B(\boldsymbol{0}, \rho_H)$ be a hyperbolic ball with large hyperbolic radius ρ_H, and Γ a discrete group of B^3-Möbius transformations (see section 2). $B(\boldsymbol{0}, \rho_H)$ is transformed by $\gamma \in \Gamma$ into a hyperbolic ball $B(\gamma\boldsymbol{0}, \rho_H)$ with Euclidean center $m_E(\gamma)$ and radius $r_E(\gamma)$ (see fig. 2). We mentioned already in the proof of (2.48) that the limit points of Γ are accumulation points of the sequence $(\gamma\boldsymbol{0})$, $\gamma \in \Gamma$. Moreover (compare the discussion of recurrence in section 1), the $\gamma\boldsymbol{0}$ approximate radially the limit points, so that for every $x \in \Lambda(\Gamma)$ the ray through $\boldsymbol{0}$ and x intersects infinitely many balls $B(\gamma\boldsymbol{0}, \rho_H)$, $\gamma \in \Gamma$ (cf. Ahlfors [3] or Beardon and Maskit [7]).

We define the shadow of a hyperbolic ball $B(\gamma\boldsymbol{0}, \rho_H)$ as its central projection from $\boldsymbol{0}$ onto the sphere at infinity (cf. Thurston [44], Ahlfors [3]). For balls $B(\gamma\boldsymbol{0}, \rho_H)$ which are sufficiently close to S_∞ we have

$$r_{cp}(\gamma) = r_E(\gamma) + \mathcal{O}\left(\left(1-\frac{|\gamma\boldsymbol{0}|^2}{R^2}\right)^2\right), \tag{4.3}$$

where $r_{cp}(\gamma)$ denotes the radius of the shadow (spherical cap on S_∞, see fig. 2).

We regard two series depending on a parameter s as equivalent $\hat{=}$ if they have with respect to s the same abscissa of convergence s_0. With the Poincaré series $h(y, s)$ defined in (2.47) (cf. also (3.13)) we can

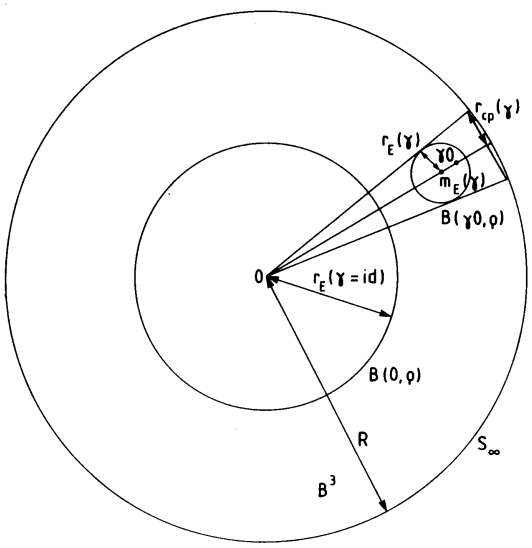

Fig. 2. Illustration of some geometric quantities introduced in section 4: Central projections of balls close to S_∞ provide Hausdorff covers for the limit set on S_∞.

now write

$$h(y=0,s) \tilde{=} \sum_{\gamma\in\Gamma} r_{cp}(\gamma)^{1+s}. \tag{4.4}$$

It is evident from the above discussion, that the central projections of the balls $B(\gamma\mathbf{0}, \rho_H)$, $\gamma \in \Gamma$, cover amply the limit set. To construct sparser covers we proceed as follows (Sullivan [41], Ahlfors [3]): We partition the balls $B(\gamma\mathbf{0}, \rho_H)$ into classes, the balls in each class having approximately the same Euclidean radius and therefore the same distance $R - |m_E(\gamma)|$ from S_∞ (provided they are sufficiently close to it), and project class after class onto S_∞. These projections constitute covers of $\Lambda(\Gamma)$ with a uniformly bounded multiplicity (Sullivan [41]). Expressed in formulae we have

$$h(y=0,s) = \sum_{\gamma\in\Gamma}\left(1-\frac{|\gamma\mathbf{0}|^2}{R^2}\right)^{1+s} = \int_0^R\left(1-\left(\frac{r}{R}\right)^2\right)^{1+s} \mathrm{d}N(r). \tag{4.5}$$

Here $N(r)$ denotes the number of $\gamma \in \Gamma$ with $|\gamma\mathbf{0}| < r$. Introducing a new dimensionless variable (cf. (4.1))

$$x = \frac{d(\mathbf{0}, r)}{R} = -\log\left(1-\frac{r^2}{R^2}\right) + \mathcal{O}(1) \tag{4.6}$$

we get

$$\begin{aligned} h(y=0,s) &\tilde{=} \int_0^\infty \mathrm{e}^{-x(1+s)}\mathrm{d}\hat{N}(x) \\ &\tilde{=} \sum_{k=1}^\infty \mathrm{e}^{-k(1+s)}\int_{k-1}^k \mathrm{d}\hat{N}(x) = \sum_{k=1}^\infty \mathrm{e}^{-k(1+s)}n(k), \end{aligned} \tag{4.7}$$

where $\hat{N}(x)$ is the number of $\gamma \in \Gamma$ with $d(\mathbf{0}, \gamma\mathbf{0})/R < x$ and $n(k)$ denotes the number of points in the shell I_k between the two hyperbolic spheres $S(\mathbf{0},(k-1)R)$ and $S(\mathbf{0}, kR)$, i.e. the number of $\gamma \in \Gamma$ satisfying

$$k-1 < \frac{d(\mathbf{0}, \gamma\mathbf{0})}{R} < k. \tag{4.8}$$

From (4.7) it follows that

$$h(y=0,s) \,\hat{\sim}\, \sum_{k=1}^{\infty} r_k^{1+s} n(k), \tag{4.9}$$

where r_k is the approximate Euclidean radius of the balls in the shell I_k (cf. (4.2), (4.6)),

$$r_k = R\tilde{c}(\rho_{\mathrm{H}}/R)\,\mathrm{e}^{-k} + \mathcal{O}(\mathrm{e}^{-2k}). \tag{4.10}$$

The Hausdorff measure on the limit set $\Lambda(\Gamma)$ is defined as follows (cf. e.g. [12], [6]): Let E be a Borel subset of $\Lambda(\Gamma)$. Define

$$m_\varepsilon^t(E) := \inf \sum_{i=1}^{\infty} r_i^t,$$

where the $r_i < \varepsilon$ are the radii of balls (spherical caps on S_∞), that constitute a countable cover of E, and the infimum is taken with respect to all such covers for a fixed $\varepsilon > 0$. Define

$$H^t(E) := \lim_{\varepsilon \to 0} m_\varepsilon^t(E).$$

Then there exists a $\delta_{\mathrm{H}} > 0$, the Hausdorff dimension, so that

$$H^t(E) = \infty \quad \text{if } t < \delta_{\mathrm{H}}$$

and

$$H^t(E) = 0 \quad \text{if } t > \delta_{\mathrm{H}}.$$

$H^{\delta_{\mathrm{H}}}(E)$ is the Hausdorff measure of E.

We assume that $0 < H^{\delta_{\mathrm{H}}}(\Lambda(\Gamma)) < \infty$ and that $H^{\delta_{\mathrm{H}}}$ measures balls of radius r centered at the limit set for $r \to 0$ as

$$H^{\delta_{\mathrm{H}}}(B(x \in \Lambda(\Gamma), r)) \,\hat{\sim}\, r^{\delta_{\mathrm{H}}}. \tag{4.11}$$

The symbol $\hat{\sim}$ means here that the ratio is bounded from above and below by positive constants. (4.11) holds even uniformly for all x (cf. Sullivan [41]); there exist two positive constants $c_{\mathrm{l.b.}}$ and $c_{\mathrm{u.b.}}$

independent of x, so that for $r \to 0$

$$c_{\text{l.b.}} < H^{\delta_H}(B(x \in \Lambda(\Gamma), r))/r^{\delta_H} < c_{\text{u.b.}}. \tag{4.12}$$

The connection between convergence abscissa s_0 of $h(y, s)$ and δ_H is established as follows: The shadows of the $n(k)$ balls (see (4.9)) with centers in the hyperbolic shell I_k (see (4.8)) cover the points of $\Lambda(\Gamma)$ with a uniformly (independent of k) bounded multiplicity. As a multiplicity bound for all I_k one can take the number m of points $\gamma \mathbf{0}$, $\gamma \in \Gamma$, in the ball $\{x | d(\mathbf{0}, x) < R\}$ which is the same as the number of the $\gamma \mathbf{0}$ in a ball $\{x | d(\tilde{\gamma}\mathbf{0}, x) < R\}$, $\tilde{\gamma} \in \Gamma$ (cf. (4.8)), because of the invariance of $d(x, y)$ under Γ (cf. (2.22), (2.24)). An argument that the multiplicity is at least one can be found in [41]. (One considers the convex hull of $\Lambda(\Gamma)$, invariant under Γ, cf. also [44].)

It follows that for $k \to \infty$

$$0 < H^{\delta_H}(\Lambda) < c_{\text{u.b.}} r_k^{\delta_H} n(k) \tag{4.13}$$

and

$$\infty > m H^{\delta_H}(\Lambda) > c_{\text{l.b.}} r_k^{\delta_H} n(k). \tag{4.14}$$

From (4.13), (4.14) we have for $k \to \infty$ (cf. [41])

$$n(k) \tilde{=} r_k^{-\delta_H} \tag{4.15}$$

and from (4.9)

$$\delta_H = 1 + s_0. \tag{4.16}$$

If we insert this into (3.15) we arrive at the formula stated in the introduction:

$$E_0 = \frac{\hbar^2}{R^2 m} \delta_H \left(1 - \frac{\delta_H}{2}\right). \tag{4.17}$$

For the numerical computation of the Hausdorff dimension the following facts are of crucial importance: We have (with $\hat{N}(k)$ and $n(l)$ as in (4.7))

$$\hat{N}(k) = \sum_{l=1}^{k} n(l). \tag{4.18}$$

From (4.10) and (4.15) we obtain for $k \to \infty$

$$n(k) \tilde{=} e^{k \cdot \delta_H} \tag{4.19}$$

and from (4.18) the same expression for $\hat{N}(k)$ (cf. Sullivan [41]),

$$\hat{N}(k) \tilde{=} e^{k \cdot \delta_H}. \tag{4.20}$$

Actually much more than (4.20) is true (cf. Lax and Phillips [25]):

$$0 < \lim_{k\to\infty} \frac{\hat{N}(k)}{e^{k\cdot\delta_H}} < \infty. \tag{4.21}$$

Taking logarithms in (4.21) we get (cf. Phillips and Sarnak [38])

$$\lim_{k\to\infty} \left[\log \hat{N}(k) - \log \hat{N}(k-1)\right] = \delta_H. \tag{4.22}$$

We had defined $\hat{N}(k)$ (cf. (4.7)) as the number of $\gamma \in \Gamma$ that satisfy

$$\frac{d(\mathbf{0}, \gamma\mathbf{0})}{R} < k. \tag{4.23}$$

If we denote by $\|\gamma\|$ the norm $(|a|^2 + |b|^2 + |c|^2 + |d|^2)^{1/2}$ of the $SL(2,\mathbb{C})$ matrix $\pm\begin{pmatrix} a & b \\ c & d \end{pmatrix}$ that is represented by the B^3-Möbius transformation γ (cf. (2.12)) we get via (2.18), (2.14) (cf. [8])

$$2\cosh \frac{d(\mathbf{0}, \gamma\mathbf{0})}{R} = \|\gamma\|^2. \tag{4.24}$$

Thus we conclude from (4.23), (4.24) that for large k $\hat{N}(k)$ is approximately the number of $\gamma \in \Gamma$ which satisfy

$$\|\gamma\|^2 < e^k. \tag{4.25}$$

Formulae (4.18)–(4.25) are the base of our Hausdorff dimension calculations in sections 7 and 8.

5. On fundamental polyhedra and deformations of hyperbolic manifolds fibering over the unit interval

In this section we work in the hyperbolic half-space model H^3. At first we recollect some concepts introduced in section 1.

A manifold $S \times]0,1[$, S a compact surface of genus two, can be represented in H^3 as a non-Euclidean fundamental polyhedron $\mathcal{F}$ of a discrete group Γ of H^3-Möbius transformations which is generated by the side-identifying transformations of $\mathcal{F}$. $S \times]0,1[$ is homeomorphic to $\mathcal{F}_M$, the hyperbolic manifold that results from identifying the sides of $\mathcal{F}$. Due to the fact that $\mathcal{F}$ is a fundamental polyhedron for Γ, the hyperbolic metric (1.1) of H^3 restricted to $\mathcal{F}$ endows $\mathcal{F}_M$ with a complete metric of constant negative curvature $-1/R^2$. The fundamental domain $\mathcal{F}$ is realized as the closure of the exterior of ten intersecting hemispheres in H^3. The base circles of these hemispheres, which lie in the plane at infinity $\mathbb{C} \cup \{\infty\}$ of H^3, as well as the identification pattern of the sides of $\mathcal{F}$ are indicated in fig. 1. The images of $\mathcal{F}$, $\gamma(\mathcal{F})$, $\gamma \in \Gamma$, tesselate H^3, and their accumulation points lie entirely on the boundary of H^3, in the interior of the ten base circles, constituting the limit set $\Lambda(\Gamma)$.

To obtain $\Lambda(\Gamma)$ it is enough to determine the accumulation points of the images $\gamma(f_1 \cup f_2)$, $\gamma \in \Gamma$, where f_1 and f_2 are the two bordering sides at infinity (hatched in fig. 1) of the polyhedron $\mathcal{F}$. We have $\mathcal{F}_M \cup f_{1,s} \cup f_{2,s} \cong S \times [0,1]$; $f_{1,s}$ and $f_{2,s}$ denote the surfaces that are obtained by identifying the boundary arcs of f_1 and likewise of f_2 as shown in fig. 1. Thus we may work in the complex plane with

non-extended Möbius transformations (1.4). The images $\gamma(f_1 \cup f_2) = \gamma(f_1) \cup \gamma(f_2)$ tesselate the whole complex plane with the exception of $\Lambda(\Gamma)$: $f_1 \cup f_2$ is a fundamental domain of Γ in $\mathbb{C} \cup \{\infty\} - \Lambda(\Gamma)$. We remark that $\Lambda(\Gamma)$ depends only on Γ and not on a special choice of the domain $\mathscr{F}$. Indeed, $\Lambda(\Gamma)$ can be defined as the set of accumulation points of the orbit γx, $\gamma \in \Gamma$, where x is any point in H^3 (cf. e.g. [26]). Replacing the circles that constitute the sides of the images $\Gamma(f_1 \cup f_2)$ by hemispheres, we get the tesselation of H^3, $\Gamma(\mathscr{F})$. Conversely, if we find ten circles as in fig. 1, so that $f_1 \cup f_2$ constitutes a fundamental domain for the group Γ, generated by the five side-identifying Möbius transformations in $\mathbb{C} \cup \{\infty\} - \Lambda(\Gamma)$, then these circles are the base circles of hemispheres that define $\mathscr{F}$ for the extended group in H^3.

We discuss now the conditions that must be fulfilled by the circles and identifying transformations in fig. 1, so that $f_1 \cup f_2$ is a fundamental domain for Γ in $\mathbb{C} \cup \{\infty\} - \Lambda(\Gamma)$. From section 1 we know that the P_i and Q_i (for the notation we refer to fig. 1) are transformed into one another via

$$P_1 \xrightarrow{T_1} P_4 \xrightarrow{T_2^{-1}} P_3 \xrightarrow{T_1^{-1}} P_2 \xrightarrow{T_2} P_5 \xrightarrow{T_5} P_1, \tag{5.1}$$

$$P_6 \xrightarrow{T_3} P_9 \xrightarrow{T_4^{-1}} P_8 \xrightarrow{T_3^{-1}} P_7 \xrightarrow{T_4} P_{10} \xrightarrow{T_5^{-1}} P_6 \tag{5.2}$$

and the same sequences with P_i replaced by Q_i. We consider only component f_1 of the fundamental domain, completely analogous results hold for f_2. From (5.1) and (5.2) we see that the vertices of f_1 are partitioned into two disjoint cycles (cf. [26]), two vertices being in the same cycle if there is a map composed of the T_i that transforms one into the other. From (5.1) it follows that the vertices P_5, P_2, P_3, P_4 are mapped into P_1 by the transformations T_5, $T_5 \cdot T_2$, $T_5 \cdot T_2 \cdot T_1^{-1}$ and $T_5 \cdot T_2 \cdot T_1^{-1} \cdot T_2^{-1}$. If the images of f_1 under these angle-preserving transformations assemble around P_1 as in fig. 3, completely covering the neighbourhood of P_1 without overlaps, we have for the angles α_i at the vertices P_i the condition

$$\sum_{i=1}^{5} \alpha_i = 2\pi. \tag{5.3}$$

Moreover we have from fig. 3 and the fact that a Möbius transformation is uniquely determined by the

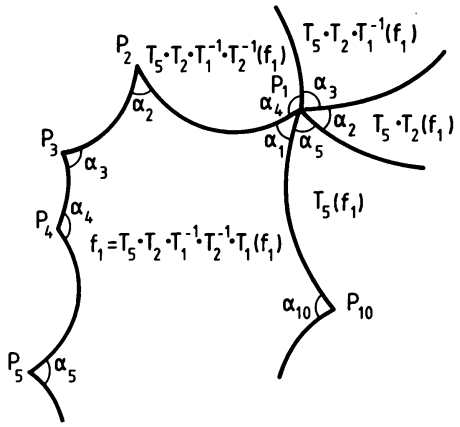

Fig. 3. Construction of a tesselation of the plane at infinity in section 5: Assemblage of images of f_1 around vertex P_1 covering its neighbourhood.

images of three points in $\mathbf{C} \cup \{\infty\}$ the relation

$$T_5 \cdot T_2 \cdot T_1^{-1} \cdot T_2^{-1} \cdot T_1 = \mathrm{id}. \tag{5.4}$$

If we had chosen another vertex instead of P_1 but in the same cycle as P_1, we would have arrived at a relation conjugated to (5.4) and at the same angle condition (5.3). For component f_2 of the fundamental domain that encloses the point at infinity, but is otherwise analogous to f_1, we derive at Q_1 the same relations (5.3) (with the same angles α_i at Q_i) and (5.4).

Turning back to f_1 we get for the second cycle (5.2) the angle relation

$$\sum_{i=6}^{10} \alpha_i = 2\pi \tag{5.5}$$

and the relation at P_6,

$$T_5^{-1} \cdot T_4 \cdot T_3^{-1} \cdot T_4^{-1} \cdot T_3 = \mathrm{id}. \tag{5.6}$$

It is clear that the angle relations (5.3) and (5.5) are a consequence of the relations (5.4) and (5.6).

There is another point that needs attention. A Möbius transformation is already uniquely determined by the images of three points in $\mathbf{C} \cup \{\infty\}$ (cf. e.g. [17]). From (5.1) we see that T_1 maps P_1 into P_4, P_2 into P_3, Q_1 into Q_4, and Q_2 into Q_3. All the other transformations must also map four given points into four given points. The ten circles in fig. 1 have to be chosen very carefully so that their intersection points Q_i, P_i can be identified according to (5.1), (5.2) by Möbius transformations T_i, which in addition have also to satisfy relations (5.4) and (5.6). It is only then that $f_1 \cup f_2$ constitutes a fundamental domain for the group Γ generated by the T_i.

We call two hyperbolic manifolds $\mathscr{F}_{\mathrm{M}}^1$, $\mathscr{F}_{\mathrm{M}}^2$ equivalent if they are isometric and the isometry arises by continuously deforming one into the other, cf. [2, 1] (Technically: we have two homeomorphisms h_1: $S \times]0,1[\to \mathscr{F}_{\mathrm{M}}^1$, h_2: $S \times]0,1[\to \mathscr{F}_{\mathrm{M}}^1$ and the isometry is homotopic to $h_1 \cdot h_2^{-1}$, cf. [10, 14]). This equivalence can be characterized in terms of the groups Γ^1, Γ^2 associated to $\mathscr{F}_{\mathrm{M}}^1$, $\mathscr{F}_{\mathrm{M}}^2$ (cf. Bers [9, 11]; Marden [28, 29]): $\Gamma^1 = \gamma \Gamma^2 \gamma^{-1}$, $\gamma \in \mathrm{SL}(2, \mathbf{C})$.

An interesting question is, how many inequivalent hyperbolic manifolds homeomorphic to $S \times]0,1[$ do exist. It can be answered at least locally, by constructing all inequivalent manifolds "near" a given one (cf. Bers [9]): Let Γ^0 be a discrete group of Möbius transformations with generators T_i^0, $i = 1, \ldots, 5$, satisfying relations (5.4) and (5.6). We call a group Γ "near Γ^0" if it has generators T_i that satisfy also relations (5.4) and (5.6) and are near T_i^0 in the sense of $\mathrm{SL}(2, \mathbf{C})$ matrix norm (see (4.24)): $\min(\|T_i^0 - T_i\|, \|T_i^0 + T_i\|)$ shall be small.

The answer is (cf. Bers [9]): All groups Γ which are sufficiently near Γ^0 and which are not conjugated to Γ^0 can be parametrized by six independent complex parameters. (This number depends only on the genus g of the compact fiber S; it is $6g - 6$.) By continuously deforming $\mathscr{F}^0$, the fundamental polyhedron of Γ^0, one can generate these groups near Γ^0.

6. On the construction of fundamental polyhedra

We describe now three techniques to construct fundamental domains in the plane at infinity, whose associated fundamental polyhedra in H^3 give rise to hyperbolic manifolds homeomorphic to $S \times]0,1[$, as

was extensively explained at the beginning of section 5. These methods will be combined in section 8 to provide examples for hyperbolic manifolds and their limit sets.

By the first method (cf. [26]) we construct a fundamental domain as in fig. 1 whose identifying transformations generate a group Γ_F with a circle as limit set.

By the second method (Thurston's Mickey Mouse, cf. [44]) we construct a non-perturbative deformation Γ_{QF} of Γ_F, its fundamental domain and its limit set which is now a directed, closed, fractal Jordan curve, sometimes resembling Mickey Mouse heads (see plate 7).

By the third method (cf. Bers [9]) we obtain various points in the deformation spaces (cf. the end of section 5) of the hyperbolic manifolds constructed by the above two methods.

In this section we work exclusively in the complex plane $\mathbb{C} \cup \{\infty\}$, the plane at infinity of H^3. The elements of a discrete group Γ we regard either as matrices in $SL(2,\mathbb{C})$ determined up to a sign, or as Möbius transformations in $\mathbb{C} \cup \{\infty\}$ (cf. (1.4)).

I. Method

We consider the subgroup of all Möbius transformations in $\mathbb{C} \cup \{\infty\}$ leaving the unit circle invariant. (For an extensive theory of these transformations see [17] and [26].) This subgroup consists of $SL(2,\mathbb{C})$ matrices of the form

$$\pm\begin{pmatrix} a & \bar{b} \\ b & \bar{a} \end{pmatrix}, \quad |a|^2 - |b|^2 = 1, \tag{6.1}$$

corresponding to $z \to (az + \bar{b})/(bz + \bar{a})$.

These transformations leave also the unit disc U: $|z| < 1$ invariant and preserve there the hyperbolic metric

$$ds^2 = \frac{4|dz|^2}{1 - |z|^2}. \tag{6.2}$$

The geodesics with respect to this metric are segments of circles orthogonal to the unit circle. Given two directed geodesics g_1, g_2 that have the same hyperbolic length, there exists a unique Möbius transformation γ of the form (6.1) that maps g_1 onto g_2 and their initial points into each other.

To construct a fundamental domain as indicated in fig. 1, we draw two circles with radii r_1 and r_2 centered at the origin of U. On each circle we place one cycle of vertices (cf. (5.1), (5.2)) in such a way (see fig. 4) that the ten vertices P_i of the component f_1 (cf. section 5 and fig. 1) of the fundamental domain are assembled in counter-clockwise order around the origin, and that the angles β_i in fig. 4 are the same if they belong to identified sides of f_1. Then we draw (see fig. 4) through each vertex pair (P_k, P_{k+1}) the circle orthogonal to the unit circle. Without changing the angles β_i we vary now the radii r_1 and r_2, $0 < r_i < 1$, to satisfy the two angle relations in (5.3), (5.5), which amounts to solving a system of two nonlinear equations in r_1 and r_2. It follows by symmetry that the arcs to be identified (see fig. 1) have not only equal Euclidean but also equal hyperbolic length. Thus the identifying Möbius transformations T_i are uniquely determined via (5.1), (5.2) and the requirement that they should be of the form (6.1). The vertices Q_i of f_2 (fig. 1) are also properly identified by these transformations, which can easily be seen by applying Ford's theory of isometric circles (cf. Ford [17]). The two relations (5.4) and (5.6) are satisfied if the angle relations are: We

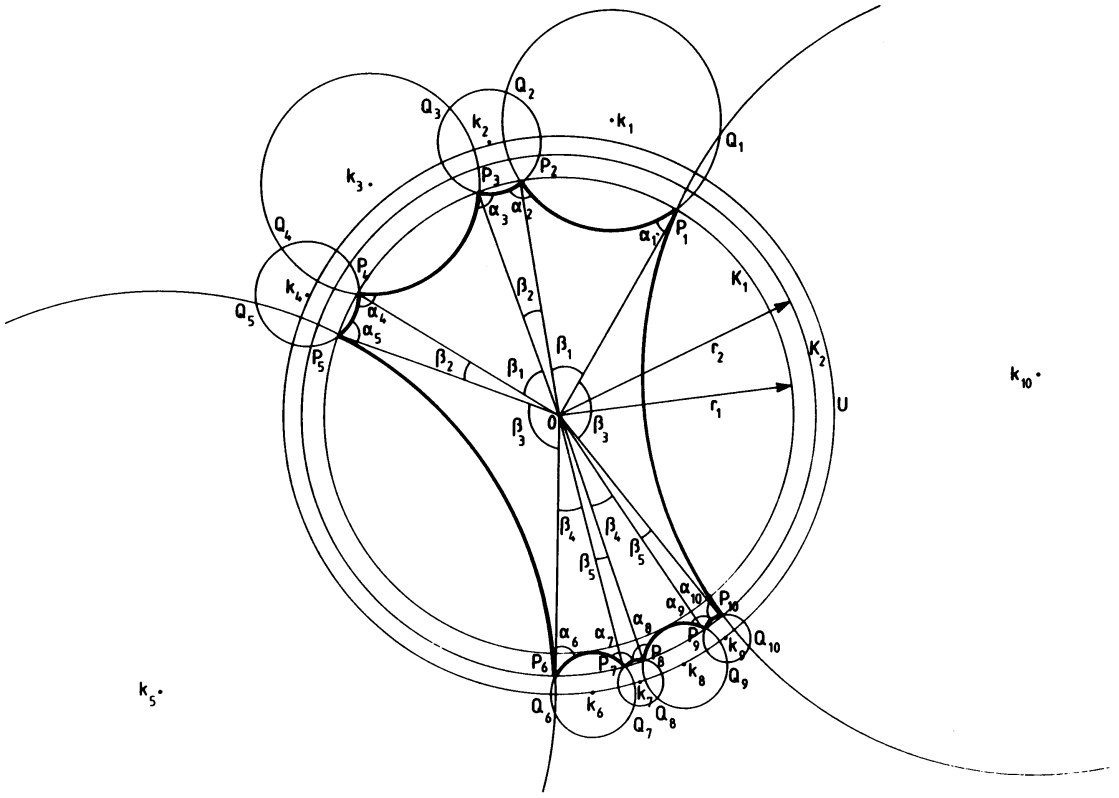

Fig. 4. Construction of a fundamental domain via Method I of section 6.

know from (5.1) that

$$T_5 \cdot T_2 \cdot T_1^{-1} \cdot T_2^{-1} \cdot T_1 P_1 = P_1.$$

If the angle relation (5.3) is satisfied, the above transformation maps the arc (P_2, P_1) onto an arc (P_2', P_1) that encloses angle zero with (P_2, P_1) at P_1. This arc is a geodesic and therefore an arc of a circle orthogonal to the unit circle. For the geodesic (P_2', P_1) has the same length as (P_2, P_1), P_2' coincides with P_2. A Möbius transformation of the form (6.1) fixing two points in U is the identity.

The limit set of the group Γ generated by the T_i lies on the unit circle, for the limit points are accumulation points of both the images $\Gamma(f_1)$ and $\Gamma(f_2)$ (cf. section 5), and Γ preserves the exterior and interior of the unit circle. In fact it can be shown that $\Lambda(\Gamma)$ is the whole unit circle (cf. [26]).

II. Method

At first we collect some facts about fixed points and multipliers of Möbius transformations in $\mathbb{C} \cup \{\infty\}$ (cf. Ford [17]).

Given a transformation $z \to (az + b)/(cz + d)$, $ad - bc = 1$, one finds immediately for the fixed points ξ_1, ξ_2:

$$\xi_{1,2} = \frac{a - d \pm \sqrt{M}}{2c}, \quad M = (a + d)^2 - 4. \tag{6.3}$$

There is only one fixed point if $M = 0$, but we will not encounter such transformations. If $c = 0$ we find in the extended plane $\mathbb{C} \cup \{\infty\}$ $\xi_1 = \infty$, $\xi_2 = b/(d - a)$, but we will also not consider such transformations. From (6.3) we have the useful formulas

$$\xi_1 + \xi_2 = \frac{a - d}{c} \tag{6.4}$$

and

$$\xi_1 \cdot \xi_2 = -\frac{b}{c}. \tag{6.5}$$

Two Möbius transformations commute with each other if and only if they have the same fixed points (cf. [26]). Every Möbius transformation γ depends on three independent complex parameters (a, b, c, d, $ad - bc = 1$). For a parametrization one can therefore use the two fixed points and the trace of the corresponding SL(2, $\mathbb{C}$) matrix (determined up to a sign), which is of course a conjugation invariant. Another conjugation invariant, for it depends only on the trace of γ, is the multiplier (or modul) K, which measures the change of scale and direction at the fixed points (cf. Ford [17]). We have

$$\frac{1}{K} + K = (a + d)^2 - 2. \tag{6.6}$$

The geometric properties of a transformation γ depend crucially on K, e.g. if K is real or $|K| = 1$ then (and only then) there exists a disc (or a half-plane) that is left invariant by γ. For the circles fixed by γ, the circles orthogonal to all of them, the isometric circle of γ, their dependence on K, and their location with respect to the fixed points and the invariant disc of γ we refer strongly to Ford [17]. We mention also that the bordering circles of the fundamental domain $f_1 \cup f_2$ constructed by Method I are the isometric circles of the transformations and their inverses by which they are identified. The modul of these transformations is real and not equal ± 1.

To construct Thurston's Mickey Mouse we start either with the fundamental domain $f_1 \cup f_2$ and the group Γ (generated by T_i, $i = 1, \ldots, 5$) obtained by Method I (see fig. 4), or with any other group conjugated to it by a Möbius transformation α that preserves the unit disc: $\Gamma \to \alpha\Gamma\alpha^{-1}$, $T_i \to \alpha T_i \alpha^{-1}$, $f_1 \cup f_2 \to \alpha(f_1 \cup f_2)$ (see fig. 5; in the following we denote the α-transformed quantities also with Γ, T_i, $f_1 \cup f_2$).

We choose a Möbius transformation γ that commutes with T_5 (and has therefore the same fixed points as T_5). γ shall not preserve the unit disc; in addition the modul K of γ shall satisfy (for geometric reasons explained later) $\mathrm{Im}(K) \neq 0$, $|K| = 1$.

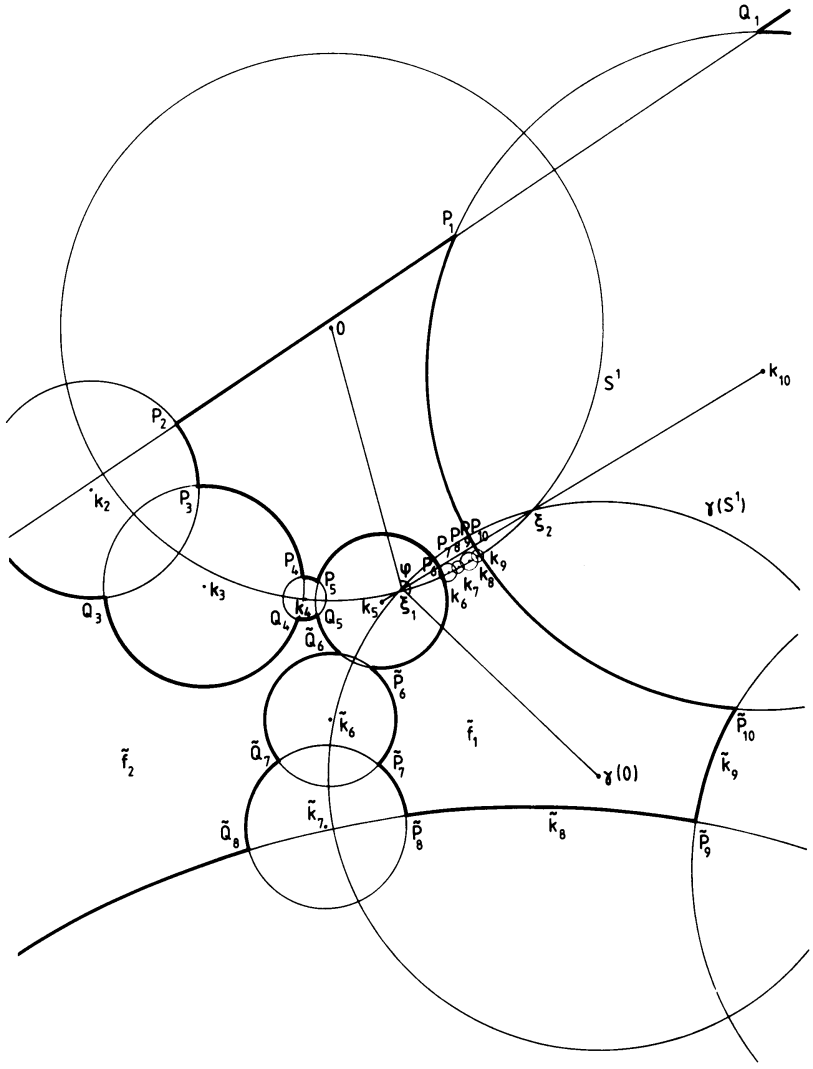

Fig. 5. Same as fig. 4, via Method II.

We define the generators of the deformed group $\tilde{\Gamma}$ as

$$\tilde{T}_i := T_i, \qquad i = 1,2;$$

$$\tilde{T}_i := \gamma T_i \gamma^{-1}, \quad i = 3,4,5.$$

Relations (5.4) and (5.6) are also satisfied by the $\tilde{T}_i$, for

$$\tilde{T}_5 = \gamma T_5 \gamma^{-1} = T_5.$$

Observe that the two fixed points ξ_1, ξ_2 of T_5 (see fig. 5) are the common intersection points of all circles orthogonal to both k_5 and k_{10}, the two circles that are identified by T_5 in fig. 1. Therefore they are also the

intersection points of the unit circle S^1 (that borders the invariant disc of T_5) with the straight line connecting the centers of k_5 and k_{10} (fig. 5). Due to its modul K γ fixes circles that are orthogonal to all circles through its fixed points, and therefore γ leaves k_5 and k_{10} invariant.

With these preparations it is easy to check that a fundamental domain $\tilde{f}_1 \cup \tilde{f}_2$ for $\tilde{\Gamma}$ is given by the vertices $\tilde{P}_i$, $\tilde{Q}_i$ defined by $\tilde{P}_i := P_i$, $\tilde{Q}_i := Q_i$ for $i = 1,\ldots,5$ and $\tilde{P}_i := \gamma P_i$, $\tilde{Q}_i := \gamma Q_i$ for $i = 6,\ldots,10$. In fig. 5 we have also drawn the image $\gamma(S^1)$ of the unit circle S^1, and we have indicated the argument φ of the modul $K = \exp(i\varphi)$ of γ. From the above it is clear that $\tilde{P}_6, \tilde{Q}_6$ and $\tilde{P}_{10}, \tilde{Q}_{10}$ are still lying on k_5 and k_{10}, and that the $\tilde{T}_i$ identify the vertices $\tilde{P}_i$ and $\tilde{Q}_i$ properly according to (5.1) and (5.2). Furthermore the $\tilde{T}_i$ have the same moduli as the T_i, for they cannot be changed by a conjugation.

The limit set $\Lambda(\tilde{\Gamma})$ of the group $\tilde{\Gamma}$ is a closed Jordan curve of fractal dimension, homeomorphic to the unit circle (the limit set of Γ). For an analytic theory of such group deformations in terms of quasiconformal mappings and Teichmüller spaces we refer to Ahlfors [2] and Bers [10, 11].

III. Method

By this method we obtain deformations of a discrete group Γ and its associated hyperbolic manifold $\mathscr{F}_M$ as indicated at the end of section 5. We parametrize all groups $\tilde{\Gamma}$ that are near and non-conjugated to a given group Γ by six independent complex parameters and construct the corresponding deformations of the fundamental polyhedron $\mathscr{F}$ of Γ via deformations of the fundamental domain $f_1 \cup f_2$ in the complex plane.

We denote the generators of Γ by T_i, $i = 1,\ldots,5$; the fixed points of T_1 by ξ_1^1, ξ_1^2 and those of T_2 by ξ_2^1, ξ_2^2. Following Bers (cf. [9]) we construct a Möbius transformation C: $z \to C(z) = (c_{11}z + c_{12})/(c_{21}z + c_{22})$, $c_{11}c_{22} - c_{21}c_{12} = 1$, satisfying the conditions $C(\xi_2^1) = 0$, $C(\xi_2^2) = \infty$, $C(\xi_1^1) \cdot C(\xi_1^2) = -1$ (cf. (6.5)). It is evident that by these conditions C is determined up to a sign, apart from the fact that it also depends on which of the two fixed points of T_2 we call ξ_2^1.

In terms of the fixed points ξ_1^1, ξ_1^2 and ξ_2^1, ξ_2^2 we have for the coefficients of $C(z)$

$$
\begin{aligned}
c_{22} &= \left[\frac{-(\xi_2^1 - \xi_1^1)(\xi_2^1 - \xi_1^2)}{(\xi_2^2 - \xi_1^1)(\xi_2^2 - \xi_1^2)} \frac{(\xi_2^2)^4}{(\xi_2^1 - \xi_2^2)^2} \right]^{1/4}, \\
c_{11} &= \frac{-\xi_2^2}{(\xi_2^1 - \xi_2^2)} \frac{1}{c_{22}}, \\
c_{12} &= \frac{\xi_2^1 \cdot \xi_2^2}{(\xi_2^1 - \xi_2^2)} \frac{1}{c_{22}}, \\
c_{21} &= -\frac{c_{22}}{\xi_2^2}.
\end{aligned}
\tag{6.7}
$$

We fix C by choosing e.g. the principal value in the expression for c_{22} in (6.7).

We pass now to SL(2, $\mathbb{C}$) matrices (cf. section 1) and choose for each of the T_i and C one of the two SL(2, $\mathbb{C}$) matrices (differing only by a sign) that represent them. We denote these matrices with the same

letters T_i, C. Relations (5.4) and (5.6) read as matrix products ($\mathrm{id} := \left(\begin{smallmatrix} 1 & 0 \\ 0 & 1 \end{smallmatrix}\right)$)

$$T_5 T_2 T_1^{-1} T_2^{-1} T_1 = \pm \mathrm{id}, \tag{6.8}$$

$$T_5^{-1} T_4 T_3^{-1} T_4^{-1} T_3 = \pm \mathrm{id}, \tag{6.9}$$

where the signs in front of id must be chosen appropriately, depending on the above choice of the $\mathrm{SL}(2,\mathbb{C})$ matrices.

If we conjugate T_2 and T_1^{-1} with C we have

$$CT_2C^{-1} = \begin{pmatrix} t & 0 \\ 0 & t^{-1} \end{pmatrix}, \quad t \in \mathbb{C} \tag{6.10}$$

and

$$CT_1^{-1}C^{-1} = \begin{pmatrix} a & b \\ b & d \end{pmatrix}, \quad ad - b^2 = 1; \quad a, b, d \in \mathbb{C}. \tag{6.11}$$

Conjugating relation (6.8) with C we get

$$\begin{pmatrix} 1 + (1-t^2)b^2 & ab(t^2-1) \\ db(t^{-2}-1) & 1 - (t^{-2}-1)b^2 \end{pmatrix} = \pm C^{-1} T_5^{-1} C, \tag{6.12}$$

with an appropriate choice of sign. From (6.11) we have also

$$ad - b^2 = 1. \tag{6.13}$$

Denoting $\pm C^{-1} T_5 C$ by (α_{ij}) $i = 1,2$; $j = 1,2$ we have from (6.12) and (6.13)

$$\begin{aligned} t &= \left[-\frac{(\alpha_{11}-1)}{(\alpha_{22}-1)} \right]^{1/2}, \\ b &= \left[\frac{(\alpha_{11}-1)(\alpha_{22}-1)}{(\alpha_{11}-1)+(\alpha_{22}-1)} \right]^{1/2}, \\ a &= \frac{-(\alpha_{22}-1)\alpha_{12}}{[(\alpha_{22}-1)+(\alpha_{11}-1)]b}, \\ d &= \frac{-(\alpha_{11}-1)\alpha_{21}}{[(\alpha_{22}-1)+(\alpha_{11}-1)]b}. \end{aligned} \tag{6.14}$$

We stress once more that the right choice of sign in (6.12) is essential to get from (6.14) via (6.10) and (6.11) the original generators.

To construct a deformation we replace T_5 in (6.12) by a matrix $\tilde{T}_5$ that is near T_5: $\|T_5 - \tilde{T}_5\|$ is small ($\|\ \|$ denotes $\mathrm{SL}(2,\mathbb{C})$ norm, cf. the end of section 4). Then we solve (6.12), (6.13). We denote the unique (in

terms of Möbius transformations) solution (6.14) by $(a_{\mathrm{I}}, b_{\mathrm{I}}, d_{\mathrm{I}}, t_{\mathrm{I}})$, which determines according to (6.10) and (6.11) the deformations $\tilde{T}_1$ and $\tilde{T}_2$ of T_1 and T_2, which satisfy together with $\tilde{T}_5$ the same relation (6.8) as the T_i,

$$\tilde{T}_2 = C^{-1}\begin{pmatrix} t_{\mathrm{I}} & 0 \\ 0 & t_{\mathrm{I}}^{-1} \end{pmatrix} C, \tag{6.15}$$

$$\tilde{T}_1 = C\begin{pmatrix} d_{\mathrm{I}} & -b_{\mathrm{I}} \\ -b_{\mathrm{I}} & a_{\mathrm{I}} \end{pmatrix} C^{-1}. \tag{6.16}$$

The second relation (6.9) we handle likewise: Let ξ_3^1, ξ_3^2 and ξ_4^1, ξ_4^2 be the fixed points of T_3 and T_4 and D a Möbius transformation, so that $D(\xi_4^1) = 0$, $D(\xi_4^2) = \infty$, $D(\xi_3^1) \cdot D(\xi_3^2) = -1$ (see (6.7) for explicit formulas). After conjugating T_4 and T_3^{-1} with D (cf. (6.10), (6.11)), we end up with equations analogous to (6.12), (6.13), with $\pm D^{-1}T_5 D$ instead of $\pm C^{-1}T_5^{-1}C$. Now we replace in these equations T_5 by $\beta\tilde{T}_5\beta^{-1}$, β being a $\mathrm{SL}(2,\mathbf{C})$ matrix near the identity, but otherwise arbitrary. Denoting their solution (cf. (6.14)) by $(a_{\mathrm{II}}, b_{\mathrm{II}}, d_{\mathrm{II}}, t_{\mathrm{II}})$ we get the deformations $\tilde{T}_3$ and $\tilde{T}_4$ of T_3 and T_4,

$$\tilde{T}_4 = \beta D^{-1}\begin{pmatrix} t_{\mathrm{II}} & 0 \\ 0 & t_{\mathrm{II}}^{-1} \end{pmatrix} D\beta^{-1}, \tag{6.17}$$

$$\tilde{T}_3 = \beta D\begin{pmatrix} d_{\mathrm{II}} & -b_{\mathrm{II}} \\ -b_{\mathrm{II}} & a_{\mathrm{II}} \end{pmatrix} D^{-1}\beta^{-1}, \tag{6.18}$$

which satisfy together with $\tilde{T}_5$ the second generator relation (6.9).

Indeed, β depends on three complex parameters and likewise $\tilde{T}_5$. So we have parametrized relations (6.8), (6.9) by six independent complex parameters (up to an overall $\mathrm{SL}(2,\mathbf{C})$ conjugation), as was stated at the end of section 5.

Finally we construct a fundamental domain $\tilde{f}_1 \cup \tilde{f}_2$ for the group $\tilde{\Gamma}$ as a deformation of the fundamental domain $f_1 \cup f_2$ of Γ. Before we formulate the conditions which the vertices $\tilde{P}_i, \tilde{Q}_i$, $i = 1, \ldots, 10$ of $\tilde{f}_1 \cup \tilde{f}_2$ have to satisfy, we list some properties of cross-ratios. A cross-ratio λ of four points z_i in $\mathbf{C}$ can be defined as

$$\lambda(z_1, z_2, z_3, z_4) := \frac{(z_1 - z_3)(z_2 - z_4)}{(z_2 - z_3)(z_1 - z_4)}.$$

It is invariant under Möbius transformations γ: $\lambda(z_i) = \lambda(\gamma z_i)$. It is real if and only if the four points lie on a circle. By definition λ does not depend on the radius of that circle. If the four points z_i are ordered in the sequence z_1, z_2, z_3, z_4 on the circle, no matter if counter-clockwise or not, we have always $0 < \lambda < 1$. For proofs of these simple facts we refer to [8] and [36].

The conditions for the vertices $\tilde{P}_i$ and $\tilde{Q}_i$ are (cf. fig. 1 and (5.1), (5.2))

$$\lambda\big(\tilde{P}_1, \tilde{Q}_1, \tilde{T}_2^{-1}\tilde{T}_5^{-1}\tilde{P}_1, \tilde{T}_2^{-1}\tilde{T}_5^{-1}\tilde{Q}_1\big) = \tilde{\lambda}_1, \tag{6.19}$$

$$\lambda\big(\tilde{P}_1, \tilde{Q}_1, \tilde{T}_5\tilde{T}_1\tilde{P}_1, \tilde{T}_5\tilde{T}_1\tilde{Q}_1\big) = \tilde{\lambda}_2, \tag{6.20}$$

$$\lambda\big(\tilde{P}_6, \tilde{Q}_6, \tilde{T}_4^{-1}\tilde{T}_5\tilde{P}_6, \tilde{T}_4^{-1}\tilde{T}_5\tilde{Q}_6\big) = \tilde{\mu}_1, \tag{6.21}$$

$$\lambda\big(\tilde{P}_6, \tilde{Q}_6, \tilde{T}_5^{-1}\tilde{T}_3\tilde{P}_6, \tilde{T}_5^{-1}\tilde{T}_3\tilde{Q}_6\big) = \tilde{\mu}_2, \tag{6.22}$$

$$\lambda\big(\tilde{P}_1, \tilde{Q}_1, \tilde{T}_5\tilde{P}_6, \tilde{T}_5\tilde{Q}_6\big) = \tilde{\nu}, \tag{6.23}$$

where $\tilde{\lambda}_i$, $\tilde{\mu}_i$ and $\tilde{\nu}$ are real and in the interval $]0,1[$. We get for each of the ten circles in fig. 1 one equation, but due to the fact that the $\tilde{T}_i$ map the circles onto one another only five equations are independent. We have to search for solutions of (6.19)–(6.23) with $\tilde{Q}_i$, $\tilde{P}_i$, $\tilde{\lambda}_i$, $\tilde{\mu}_i$, $\tilde{\nu}$ near the unperturbed Q_i, P_i, λ_i, μ_i, ν. (The last three quantities are defined by (6.19)–(6.23) with vertices and generators replaced by the unperturbed ones.)

At first we choose a $\tilde{P}_1$ near P_1. Then we solve analytically (6.19) for $\tilde{Q}_1$: $\tilde{Q}_1 = f_1^{(i)}(\tilde{\lambda}_1)$, $i = 1,2$ (The index i denotes the two branches of the solution). This expression for $\tilde{Q}_1$ we insert into (6.20). The imaginary part of this equation depends therefore only on $\tilde{\lambda}_1$. Solving this equation numerically for $\tilde{\lambda}_1$ (actually there are two equations to scan for solutions, one for each branch of $f_1^{(i)}$) we get also $\tilde{\lambda}_2$ and $\tilde{Q}_1$. (There are of course many solutions, we choose one that is near λ_1, λ_2 and Q_1, moreover $\tilde{\lambda}_1$ and $\tilde{\lambda}_2$ must be in the interval $]0,1[$.)

Next we choose a $\tilde{\nu}$ near ν and calculate $\tilde{P}_6$ and $\tilde{Q}_6$ from (6.21)–(6.23) as follows: At first we express analytically $\tilde{Q}_6$ via (6.23) as a function of $\tilde{\mu}_1$ and $\tilde{P}_6$: $\tilde{Q}_6 = f_2^{(i)}(\tilde{P}_6, \tilde{\mu}_1)$, $i = 1,2$ (i denotes branches). This expression we insert into (6.22); the resulting equation is equivalent to the problem of finding the roots of a third order polynomial in $\tilde{P}_6$. This is done analytically: $\tilde{P}_6 = f_3^{(i),(k)}(\tilde{\mu}_1)$, $i = 1,2$; $k = 1,2,3$. Inserting the expressions for $\tilde{P}_6$ and $\tilde{Q}_6$ into (6.21) and taking the imaginary part, we end up with an equation for $\tilde{\mu}_1$, which we scan numerically for solutions in the interval $]0,1[$. (One has to scan six such equations, because of the branches of $f_3^{(i),(k)}$). We choose again a solution $\tilde{\mu}_1$ near μ_1, so that $\tilde{Q}_6$ and $\tilde{P}_6$ are close to Q_6 and P_6.

By applying the $\tilde{T}_i$ to $\tilde{P}_1, \tilde{Q}_1, \tilde{P}_6, \tilde{Q}_6$ we get all other vertices of the fundamental domain $\tilde{f}_1 \cup \tilde{f}_2$. The system (6.19)–(6.23) admits of course many solutions of the form indicated in fig. 1, but the hyperbolic manifolds arising from the so defined fundamental polyhedra are all equivalent (cf. the end of section 5), for they belong to the same group $\tilde{\Gamma}$.

7. On the construction of the limit set $\Lambda(T)$ and the calculation of its Hausdorff dimension

At the beginning of section 5 we have seen that $\Lambda(\Gamma)$ is just the set of accumulation points of the tesselation $\Gamma(f_1 \cup f_2)$ of the complex plane. It has been mentioned (cf. section 6) that $\Lambda(\Gamma)$ constitutes a closed Jordan curve, dividing the extended complex plane $\mathbf{C} \cup \{\infty\}$ into two connected and simply connected domains, tesselated by $\Gamma(f_1)$ and $\Gamma(f_2)$.

In the following we construct a tesselation that provides us ultimately with $\Lambda(\Gamma)$ and gives also the clue to count the $\gamma \in \Gamma$ that have a norm below a given bound (cf. (4.25)), which is the essential step in the calculation of the Hausdorff dimension.

In order to generate systematically the tesselation, more formal notation (than was used in section 5) has to be introduced: P_i^j, Q_i^j, $i=1,\dots,m_j$, denote the vertices of the jth cycle ($j=1,2$) in counter-clockwise order viewed from the interior of f_1 (see fig. 1 and section 5). T_i^j, $i=1,\dots,m_j$; $j=1,2$, denote maps composed of the identifying transformations T_i of $f_1 \cup f_2$ and their inverses (cf. (5.1), (5.2), (5.4), (5.6)) which satisfy

$$\begin{aligned} &T_i^j P_i^j = P_{i+1}^j, \quad i=1,\dots,m_j-1; \quad j=1,2; \\ &T_{m_j}^j P_{m_j}^j = P_1^j, \quad j=1,2. \end{aligned} \tag{7.1}$$

With the notation of fig. 1 and (5.1), (5.2) we have $P_i^1 := P_i$, $P_i^2 := P_{i+5}$, $i=1,\dots,5$, and the same connection between the Q_i^j and Q_i. The connection between the T_i and T_i^j is given by

$$\begin{aligned} &T_1^1 := T_2^{-1}T_5^{-1}, \quad T_2^1 := T_1, \quad T_3^1 := T_2, \quad T_4^1 := T_5^{-1}T_1^{-1}, \quad T_5^1 := T_5, \quad T_1^2 := T_4^{-1}T_5, \\ &T_2^2 := T_3, \quad T_3^2 := T_4, \quad T_4^2 := T_5T_3^{-1}, \quad T_5^2 := T_5^{-1}. \end{aligned}$$

We define $T_i^j := \mathrm{id}$ if $i \le 0$ and

$$X_{l,k}^j := T_{l-1}^j \cdot T_{l-2}^j \cdot \dots \cdot T_{l-k}^j \tag{7.2}$$

and

$$\begin{aligned} &Y_{l,k}^j := T_{m_j}^j \cdot T_{m_j-1}^j \cdot \dots \cdot T_{m_j-k+l}^j \quad \text{if } l-k \le 0, \\ &Y_{l,k}^j := \mathrm{id} \qquad\qquad\qquad\qquad\quad \text{if } l-k > 0 \end{aligned}$$

and finally

$$S_{l,k}^j := X_{l,k}^j \cdot Y_{l,k}^j, \tag{7.3}$$

with $j=1,2$; $l=1,\dots,m_j$; $k=1,\dots,m_j$ ($m_1=m_2=5$).

Then we have from (7.1)

$$\begin{aligned} &S_{l,k}^j P_{l-k}^j = P_l^j \quad \text{if } l-k>0, \\ &S_{l,k}^j P_{m_j-k+l}^j = P_l^j \quad \text{if } l-k \le 0. \end{aligned} \tag{7.4}$$

Relations (5.4) and (5.6) are satisfied if and only if

$$S_{l,m_j}^j = \mathrm{id}, \quad l=1,\dots,m_j; \quad j=1,2. \tag{7.5}$$

These equations constitute the cycle relations at the vertices P_l^j and Q_l^i. (5.4) corresponds to $S_{1,5}^1 = \mathrm{id}$, (5.6) to $S_{1,5}^2 = \mathrm{id}$, and the remaining equations in (7.5) are conjugated to them and therefore satisfied if they are.

The images of the fundamental domain $f_1 \cup f_2$ that cover the neighbourhood of the vertices P_l^j, Q_l^j are given by

$$S_{l,k}^j(f_1 \cup f_2) = S_{l,k}^j(f_1) \cup S_{l,k}^j(f_2) =: f_{1,k}^{l,j} \cup f_{2,k}^{l,j}; \tag{7.6}$$

they are disconnected just like the original domain $f_1 \cup f_2$. The order of the $f_{1,k}^{l,j}$ and $f_{2,k}^{l,j}$ (cf. fig. 3) is sometimes important: We have in counter-clockwise order around P_l^j: $f_1, f_{1,1}^{l,j}, f_{1,2}^{l,j}, \ldots, f_{1,m_j}^{l,j} = f_1$; and in clockwise order around Q_l^j: $f_2, f_{2,1}^{l,j}, f_{2,2}^{l,j}, \ldots, f_{2,m_j}^{l,j} = f_2$.

The images $f_{1,k}^{l,j}$, $j = 1,2$; $l = 1,\ldots,m_j$; $k = 1,\ldots,m_j - 1$, enclose completely f_1. Note that in this collection the images which have a side in common with f_1 (not only a vertex) appear twice. Exactly the same holds for f_2 and $f_{2,k}^{l,j}$. Thus we have thirty images of $f_1 \cup f_2$ that enclose $f_1 \cup f_2$, and each of them has at least one vertex with f_1 and one vertex with f_2 in common. We assemble these images in (counter-)clockwise order around $f_1 \cup f_2$, call them the first generation of fundamental domains $(G_n^1)_{n=1,N_1}$, $N_1 = 30$, and denote the $S_{l,k}^j$ which generated them by S_i, $i = 1,\ldots,30$; only thirty of the $S_{l,k}^j$ are different from one another and not equal to the identity:

$$S_i(G_1^0) = G_i^1, \quad i = 1,\ldots,30. \tag{7.7}$$

G_1^0 denotes $f_1 \cup f_2$, the zeroth generation.

The second generation $(G_n^2)_{n=1,N_2}$ is constituted by those images of $f_1 \cup f_2$ which have at least one vertex in common with each component of an element of the first generation and do not appear in the first or zeroth generation. The domains of the second generation are generated by applying the S_i of (7.7) to the elements of the first generation: $S_i(G_n^1)$, $i = 1,\ldots,30$; $n = 1,\ldots,30$. Many of these 900 domains are identical or appeared in a former generation. Taking this into account and selecting we get the second generation: $(G_n^2)_{n=1,N_2}$, $N_2 = 1,\ldots,630$.

The third generation $(G_n^3)_{n=1,N_3}$ is contained among the images $S_i(G_l^2)$, $i = 1,\ldots,30$; $l = 1,\ldots,630$, and to create the nth generation (defined as the collection of domains that have at least one vertex in common with the $(n-1)$th generation and do not appear in a former one) we apply S_i, $i = 1,\ldots,30$, to the domains of the $(n-1)$th generation, discard these domains that have already appeared in the $(n-2)$th, $(n-1)$th and nth generation to be created, assemble the new domains in (counter-)clockwise order around the $(n-1)$th generation, and end up with a generation $(G_j^n)_{j=1,N_n}$ in which the number of elements N_n is about $\frac{2}{3}N_{n-1}^2$.

Comparing and selecting fundamental domains means in practice to compare these $SL(2,\mathbb{C})$ matrices that generate them: To every domain D in the tesselation $\Gamma(f_1 \cup f_2)$ there belongs a $\gamma \in \Gamma$ so that $\gamma(f_1 \cup f_2) = D$. This γ, the generator of D, is unique and determines up to a sign a $SL(2,\mathbb{C})$ matrix (cf. e.g. section 1), which we call likewise the generator of D. The Euclidean area of the fundamental domains $\gamma(f_1 \cup f_2)$, $\gamma \in \Gamma$, decreases rapidly towards zero with increasing n (n means the generation index; within a given generation G^n the areas are approximately of the same size), likewise the distance between the components $\gamma(f_1)$ and $\gamma(f_2)$ decreases, localizing so the Jordan curve, and the norms $\|\gamma\|$ of the generators γ increase and tend to infinity. Note that the generators have to contract the original domain $f_1 \cup f_2$ into arbitrarily small ones, if we approach the Jordan curve.

A straightforward way to determine $\hat{N}(\lambda)$, the number of $\gamma \in \Gamma$ that satisfy (cf. (4.25))

$$\|\gamma\|^2 < e^{\lambda}, \tag{7.8}$$

would be to calculate generation after generation according to the above description and to count the matrices by applying (7.8) to every domain, but the dramatic increase of N_n with increasing n makes it virtually impossible. Therefore we implement the selection criterion (7.8) already in the definition of the generations, which get then a more tractable size determined by λ: We define the zeroth and first generations as before, so that the S_i are the same as in (7.7). For $n>2$ we define the nth generation $(G_j^{n,\lambda})_{j=1,N_{n,\lambda}}$ as the collection of domains $\gamma(f_1 \cup f_2)$, $\gamma \in \Gamma$, that (1) have at least one vertex in common with the $(n-1)$th generation, (2) do not appear in any former generation and (3) have generators that satisfy (7.8). $(G_j^{n,\lambda})_{j=1,N_{n,\lambda}}$ is created by applying as before the S_i of (7.7) to the $(n-1)$th generation and by selecting according to the three criteria just mentioned.

With this definition the number $N_{n,\lambda}$ of elements in the nth generation for a given λ will at first increase with increasing n, reach a maximum for an n depending on λ, and then decrease rapidly to zero, so that only the first few terms in the series

$$\hat{N}(\lambda) = \sum_{n=0}^{\infty} N_{n,\lambda} \tag{7.9}$$

are non-zero. The Hausdorff dimension of $\Lambda(\Gamma)$ is then calculated via (4.22) or much more efficiently via (4.21); see the "Note added in proof" and section 8.

8. How it works: Examples and conclusion

Plates I–X show the plane at infinity of hyperbolic space H^3 (cf. section 1) endowed with tesselations that originate (cf. sections 1, 5, 7 and fig. 1) as follows:

The large (black) domain in the middle of the plates is nothing but component f_1 (cf. fig. 1) of the fundamental domain $f_1 \cup f_2$ (cf. section 5) that is bordered by arcs of ten intersecting circles, which are listed for plates I, III–VI in tables I–V. Fragments of f_2, the component that encloses the point at infinity of $\mathbf{C} \cup \{\infty\}$, are likewise colored in black. The intersection points of the ten circles define via (5.1), (5.2) the side-pairing maps T_i (cf. fig. 1) for both f_1 and f_2, which get then the surfaces $f_{1,s}$, $f_{2,s}$ (cf. section 5) topologically equivalent to a sphere with two handles ("figure eight"). These surfaces constitute the two boundary components of a three-dimensional hyperbolic manifold $\mathscr{F}_M$ that can be imagined topologically as a "surface" (a handle body with two handles like above) which has a finite thickness: $\mathscr{F}_M \cong]0,1[\times f_{1,s}$ (cf. sections 1 and 5; we have removed the two bordering surfaces $f_{1,s}$ and $f_{2,s}$ at infinity of H^3, where the metric (1.1) gets singular).

$\mathscr{F}_M$ is realized in H^3 by placing hemispheres on the ten circles, which are then identified by the lifted T_i (cf. section 1) and provide together with $f_1 \cup f_2$ the boundary of the fundamental polyhedron $\mathscr{F}$ (cf. section 1) that fills the space above the ten hemispheres and $f_1 \cup f_2$ in H^3. That $\mathscr{F}_M$ is actually homeomorphic to a thickened handle body is best seen if one picks out a fundamental polyhedron in the first generation of the H^3-tesselation (see below), which has obviously finite Euclidean volume. One locates with ease the fibers of $]0,1[\times f_{1,s}$, sandwiched between the Γ-images of $f_{1,s}$ and $f_{2,s}$.

$\mathscr{F}$ is designed so that the Poincaré metric (1.1) restricted to it fits smoothly on the identified hemispheres; the requirement for this is (cf. section 1) that $\Gamma(\mathscr{F})$ tesselates H^3 (Γ is the discrete group generated by the lifted T_i). Every image $\gamma(\mathscr{F})$, $\gamma \in \Gamma$, in the tesselation of H^3 is again bordered by

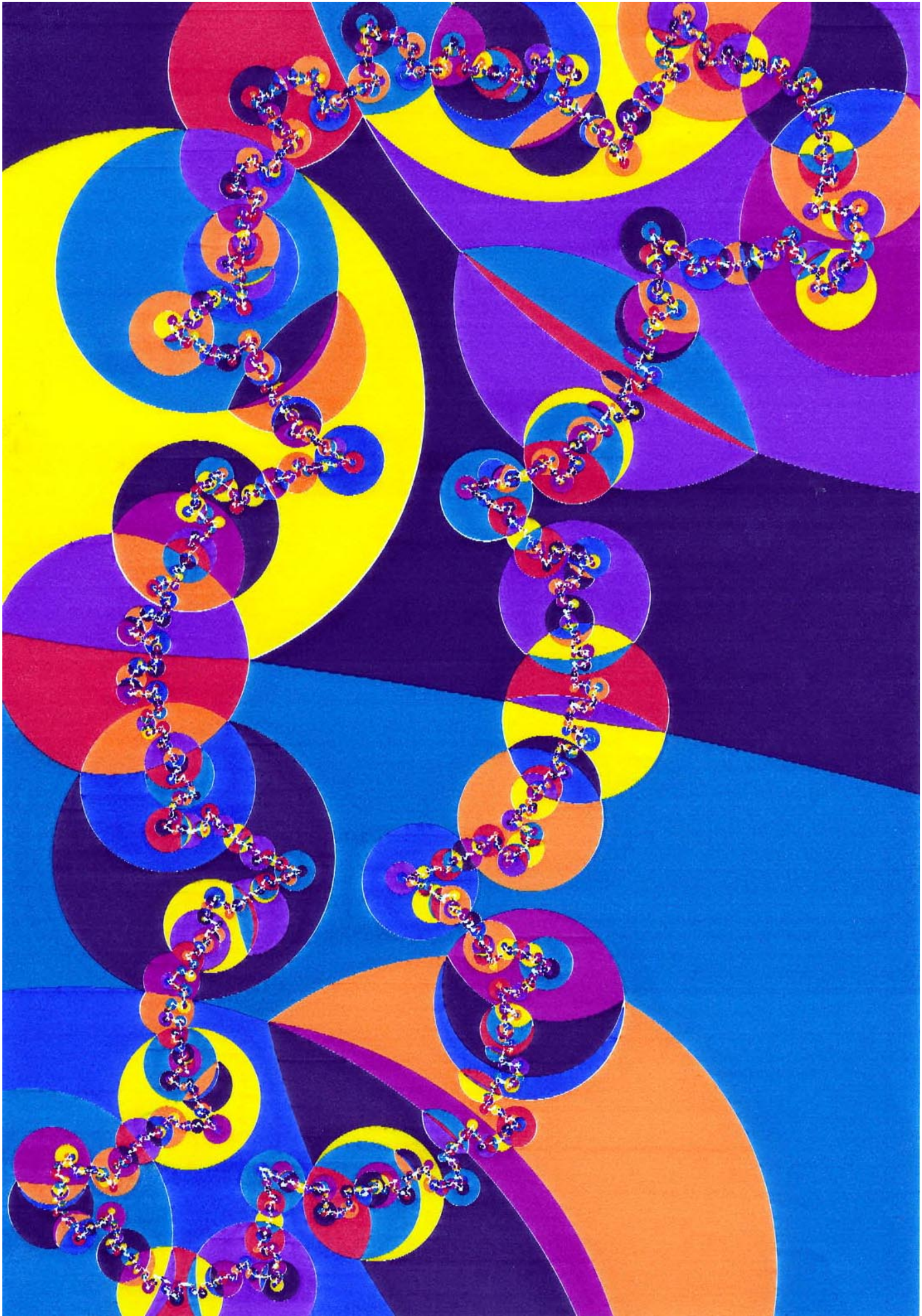

Plates I & II

(The description of the plates is given in section 8.)

Plates III & IV

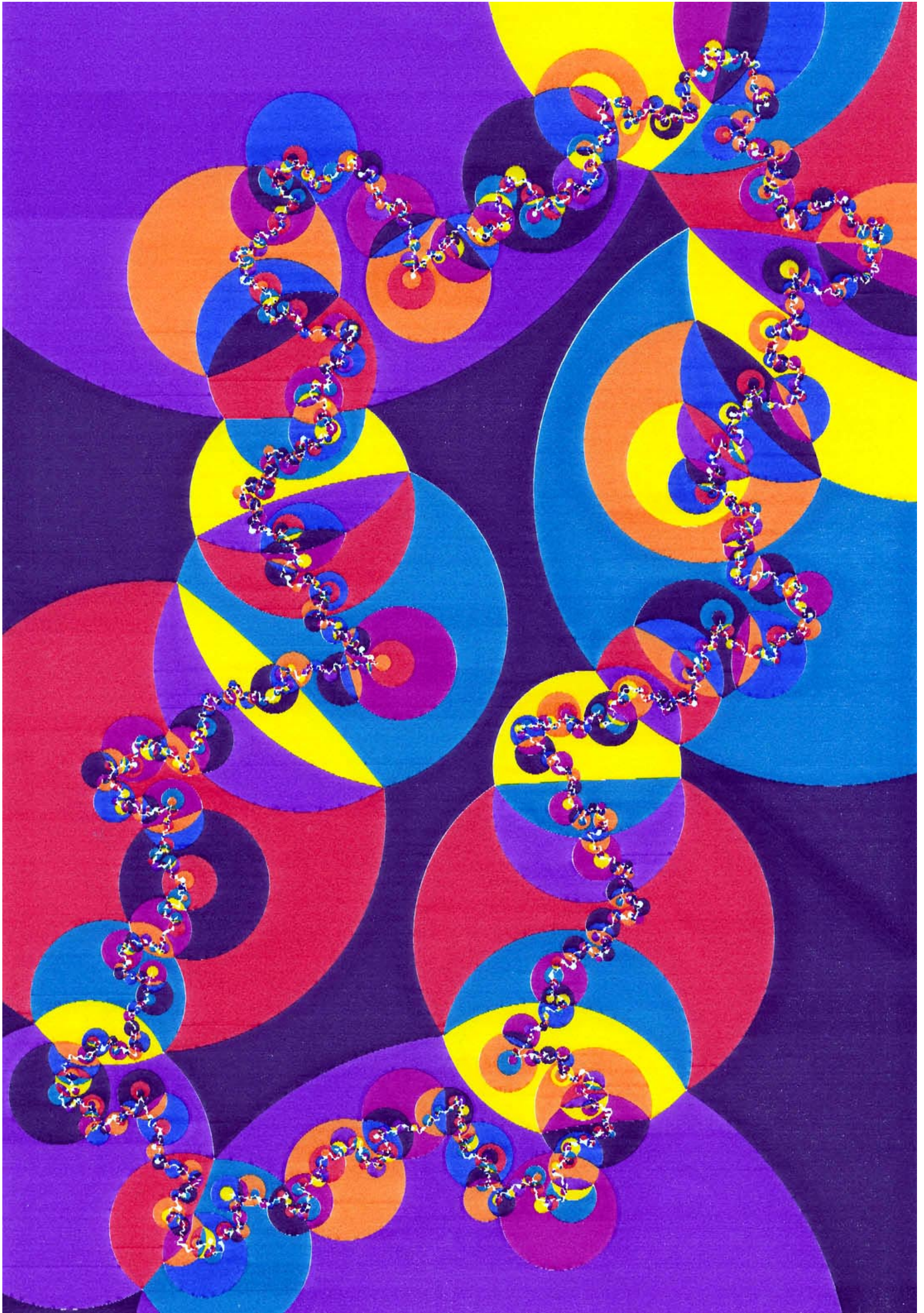

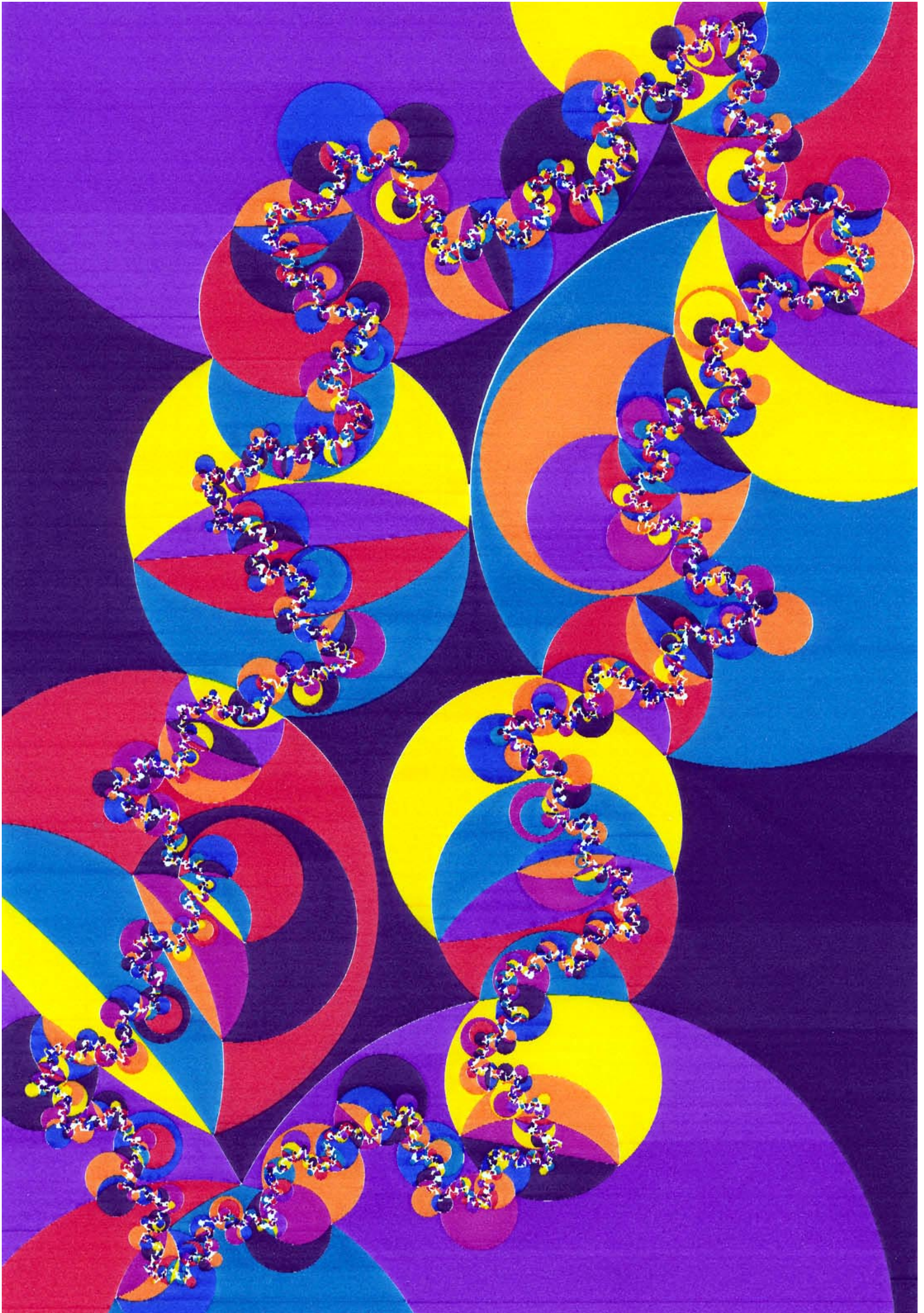

Plates V & VI

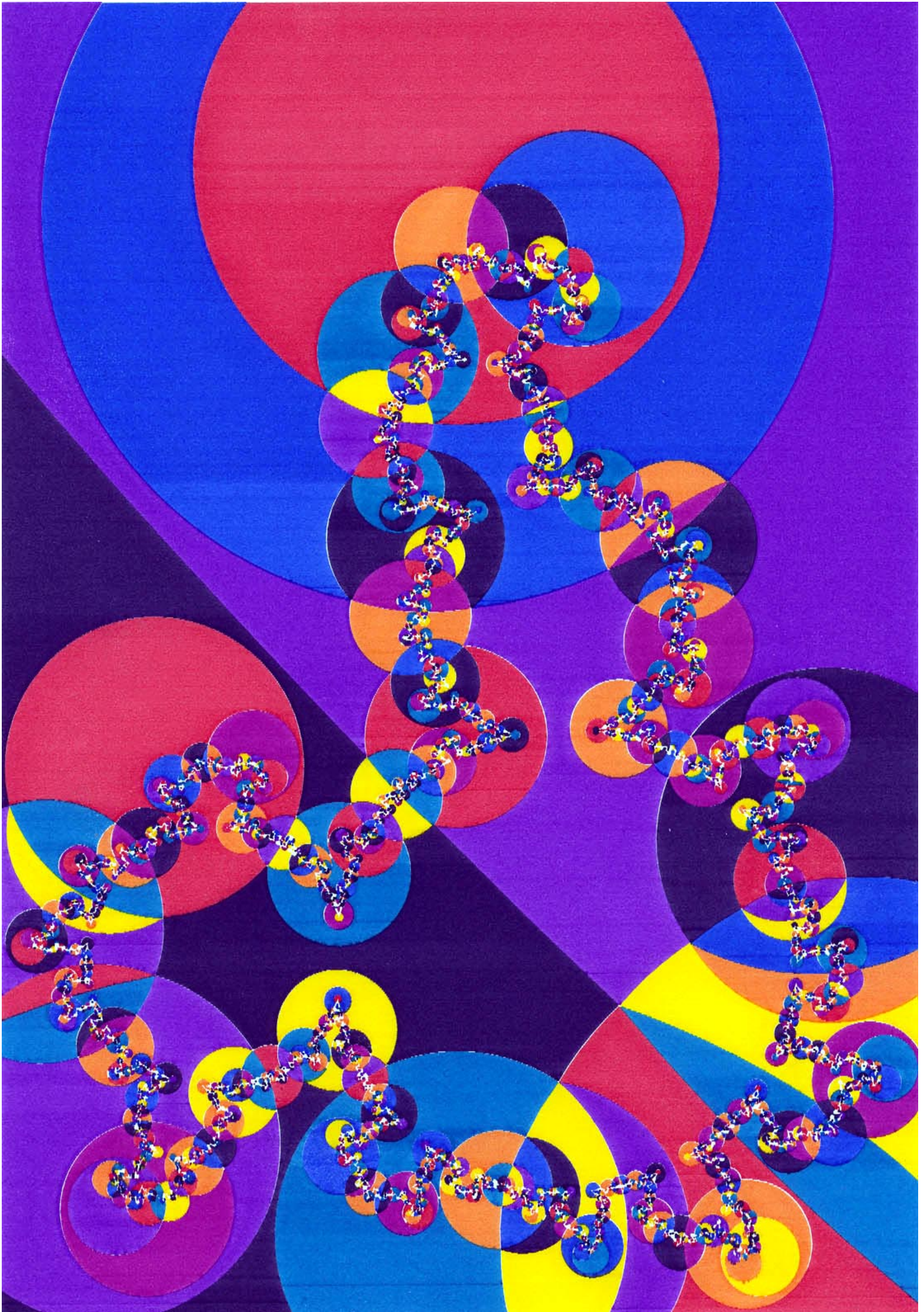

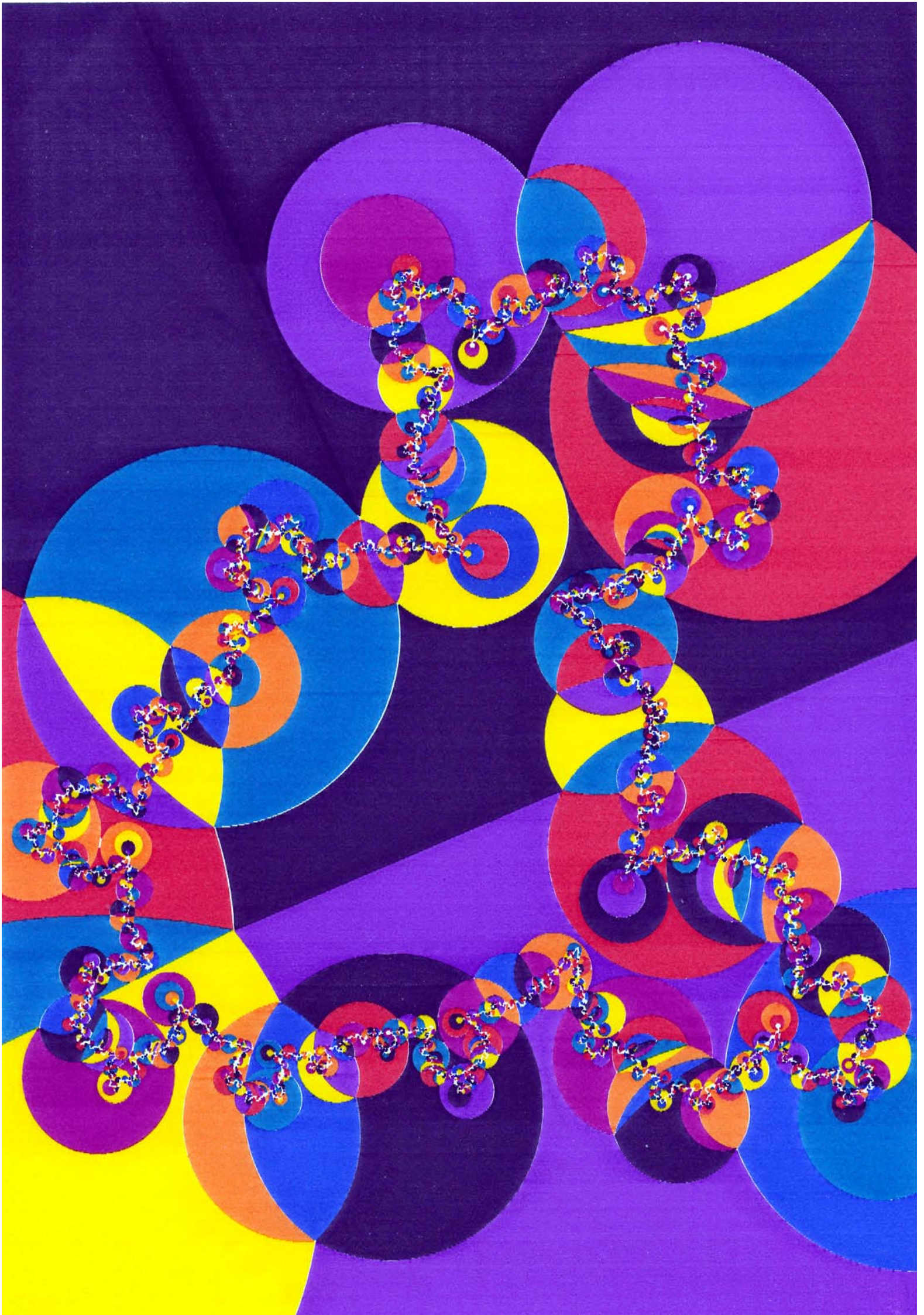

Plates VII & VIII

Plates IX & X

Table I
For plate I; we refer to section 8 for definitions and explanations.

Circles (cf. fig. 1):

	Center		Radius
k_1	−14.156514	21.808275	25.980912
k_2	−0.909954	−0.572173	0.394207
k_3	−0.498929	−0.939681	0.363222
k_4	−0.124789	−0.995978	0.086862
k_5	0.139416	−1.015044	0.223052
k_6	−0.041360	−1.438881	0.240246
k_7	0.202477	−2.217573	0.915967
k_8	0.645361	−5.387198	3.613570
k_9	2.267842	−1.833041	0.492342
k_{10}	1.633319	−0.261232	1.317563

$\delta_H = 1.237$; cf. (4.21) and the "Note added in proof"

λ	$\hat{N}(\lambda)$ (cf. (7.9))	$\log(\hat{N}(\lambda)/\hat{N}(\lambda-1))$ (cf. (4.22))
6.7	665	
7.7	2292	1.237
8.7	7944	1.243
9.7	27333	1.235
10.7	93656	1.231

Table II
For plate III; see section 8.

Circles (cf. fig. 1):

	Center		Radius
k_1	1.395552	0.586539	1.136484
k_2	0.018466	1.530282	1.158492
k_3	−2.603582	0.575934	2.471910
k_4	−0.561346	−0.855444	0.216555
k_5	−0.020540	−1.104668	0.469802
k_6	−0.594877	−1.975430	0.584454
k_7	0.552373	−3.096859	1.105434
k_8	2.650862	−3.311626	2.857903
k_9	1.216997	−1.027330	0.215777
k_{10}	0.788554	−0.700016	0.334426

$\delta_H = 1.250(5)$; cf. (4.21)

λ	$\hat{N}(\lambda)$ (cf. (7.9))	$\log(\hat{N}(\lambda)/\hat{N}(\lambda-1))$ (cf. (4.22))
5.98	324	
6.98	1236	1.338
7.98	4222	1.228
8.98	14952	1.264
9.98	52142	1.249
9.45	26918	
10.45	93970	1.250

Table III
For plate IV; see section 8.

Circles (cf. fig. 1):

	Center		Radius
k_1	0.975071	0.554298	1.079585
k_2	−0.083602	1.756191	1.169246
k_3	−1.870359	0.237139	1.553050
k_4	−0.491101	−0.822515	0.287197
k_5	−0.108278	−1.004079	0.465251
k_6	−0.330426	−1.887739	0.457742
k_7	1.376649	−3.560633	2.140116
k_8	2.838563	−3.610540	3.095167
k_9	1.203516	−0.954412	0.137922
k_{10}	0.788851	−0.789827	0.335620

$\delta_H = 1.222$; cf. (4.21)

λ	$\hat{N}(\lambda)$ (cf. (7.9))	$\log(\hat{N}(\lambda)/\hat{N}(\lambda-1))$ (cf. (4.22))
5.64	176	
6.64	666	1.331
7.64	2334	1.254
8.64	7748	1.200
9.64	26540	1.231
10.64	89052	1.210

$K = |K|e^{i\varphi}$, $|K| < 1$; cf. (6.6)
$\varphi(T_1) = 10.1°$; $\varphi(T_2) = 342.1°$; $\varphi(T_3) = 8.9°$; $\varphi(T_4) = 345.8°$; $\varphi(T_5) = 2.5°$

domains on hemispheres which have to be placed – to get the tesselation of H^3 – on the ten bordering circles of the images $\gamma(f_1 \cup f_2)$, $\gamma \in \Gamma$, colored in the plates as follows (cf. sections 5, 7): We attach around f_1 and simultaneously around f_2 the first generation of their images $\gamma(f_1)$ and $\gamma(f_2)$ respectively, i.e. all images $\gamma(f_1 \cup f_2)$, $\gamma \in \Gamma$, that have a vertex P_i (cf. fig. 1) in common with f_1 and therefore also the corresponding vertex Q_i with f_2. The domains $\gamma(f_1) \cup \gamma(f_2)$ (they are disconnected but not so the $\gamma(\mathcal{F})$ erected on them) of this generation are colored with red, turquoise, yellow and violet. The second generation attached analogously around the first has the colors black, red-violet, orange and blue. The third selective (cf. the end of section 7) generation is colored like the first, and so on.

Attaching generation after generation the limit set $\Lambda(\Gamma)$, a closed nonrectifiable Jordan curve, emerges in an obvious way as the set of accumulation points of H^3-polyhedra (cf. sections 1, 5, 7). The compact set of directed geodesics in H^3 (semicircles orthogonal to the complex plane, see section 1) with both initial and end points in $\Lambda(\Gamma)$ provides – if projected into $\mathcal{F}_M$ (cf. the end of section 1) – just the geodesics which are bounded and recurrent for $t \to \pm\infty$, and Hausdorff covers of $\Lambda(\Gamma)$ were constructed (cf. section 4) by means of a geometric interpretation of the resolvent kernel of the Schrödinger operator, relating so the Hausdorff dimension of $\Lambda(\Gamma)$ to the energy ground state (cf. (4.17)).

On plates I and II we erect by placing hemispheres on the ten bordering circles of $f_1 \cup f_2$ (cf. table I for plate I) two fundamental polyhedra, whose sides are identified by the same T_i (cf. fig. 1), giving rise to the same group Γ. The so defined manifolds are isometric, the ground state originates from the same limit set. Γ is a purely hyperbolic group, i.e. the moduli of its elements (see (6.6)) are real and not equal to ± 1. Fig.

Table IV
For plate V; see section 8.

Circles (cf. fig. 1):

	Center		Radius
k_1	0.729563	0.398527	0.934335
k_2	0.018209	2.222011	1.570288
k_3	−1.620015	0.233028	1.326035
k_4	−0.427097	−0.799830	0.351445
k_5	−0.061913	−0.994302	0.530611
k_6	−0.059027	−1.839737	0.742463
k_7	0.532809	−2.786644	0.455481
k_8	1.985536	−2.373398	1.141879
k_9	1.196149	−1.119388	0.567787
k_{10}	0.802191	−0.755710	0.295811

$\delta_H = 1.225$; cf. (4.21)

λ	$\hat{N}(\lambda)$ (cf. (7.9))	$\log(\hat{N}(\lambda)/\hat{N}(\lambda-1))$ (cf. (4.22))
6.5	606	
7.5	2124	1.254
8.5	7138	1.212
9.5	24300	1.225
9.6	27414	
10.6	92492	1.216

$K = |K|e^{i\varphi}$, $|K| < 1$; cf. (6.6) $\varphi(T_1) = 25.7°$; $\varphi(T_2) = 327.8°$; $\varphi(T_3) = 20.5°$; $\varphi(T_4) = 333.7°$; $\varphi(T_5) = 5°$

4 and fig. 5 are just the construction drawings for this group. The fundamental domains $f_1 \cup f_2$ shown in the plates were constructed, like in the following examples, via (6.19)–(6.23). The calculation of the Hausdorff dimension is shown in table I: $\delta_H = 1.237$; see also the "Noted added in proof".

The fundamental polyhedron of plate III (cf. table II) is constructed analogously: Starting with the group Γ given by the side-pairing maps T_i of fig. 4, contracting by an overall conjugation $T_i \to \gamma T_i \gamma^{-1}$, $i = 1,\ldots,5$, with a hyperbolic γ the circles identified by T_3 and T_4 (like in fig. 5, now schematic), and finally expanding these circles by conjugating the transformations of the second relation (5.6) as described in section 6 (Method II). Γ is again purely hyperbolic. The Hausdorff dimension: $\delta_H = 1.250(5)$.

Plates IV–VI (tables III–V) show three points in the deformation space (cf. the end of section 5) of the manifold of plate III. The side-identifying maps of the fundamental polyhedra of these manifolds were obtained by parametrizing relations (6.8), (6.9) by the phase of the modul of T_5 as explained in Method III of section 6. The phases of the moduli of the deformed generators T_i are listed in the tables. The Hausdorff dimensions are: δ_H (plate IV) = 1.222; δ_H (plate V) = 1.225; δ_H (plate VI) = 1.256.

Finally, plate VII represents again a manifold constructed like those of plates I–III with hyperbolic generators T_i. Turning on the phase of T_5, 2°–5°–8°, we get the deformations shown in plates VIII–X. The Hausdorff dimensions are

δ_H (plate VII) = 1.287(5); δ_H (plate VIII) = 1.252; δ_H (plate IX) = 1.234; δ_H (plate X) = 1.263.

It would be nice to explore (graphically) the deformations close to the boundary of Teichmüller space [9, 18, 44, 45, 24, 58], and to calculate δ_H there. First experiments in this direction have already been carried through [47].

Table V
For plate VI; see section 8.

Circles (cf. fig. 1):

	Center		Radius
k_1	0.574526	0.207802	0.838125
k_2	0.138942	1.969841	1.265019
k_3	−1.415728	0.341493	1.145613
k_4	−0.345458	−0.789245	0.518202
k_5	−0.250640	−0.867892	0.506530
k_6	0.170748	−1.967797	0.714917
k_7	0.140781	−5.199613	2.982464
k_8	1.954467	−2.010068	1.036171
k_9	1.042618	−1.080627	0.367640
k_{10}	0.829045	−0.962785	0.448113

$\delta_H = 1.256$; cf. (4.21)

λ	$\hat{N}(\lambda)$ (cf. (7.9))	$\log(\hat{N}(\lambda)/\hat{N}(\lambda-1))$ (cf. (4.22))
6.35	634	
7.35	2148	1.220
8.35	7774	1.286
9.35	27263	1.255
10.35	94981	1.248

$K = |K|e^{i\varphi}$, $|K| < 1$; cf. (6.6)
$\varphi(T_1) = 44.8°$; $\varphi(T_2) = 316.0°$; $\varphi(T_3) = 365.1°$; $\varphi(T_4) = 322.6°$; $\varphi(T_5) = 8°$

I conclude with some remarks to formula (0.1). Referring to the end of section 1, δ_H turns out to be a measure for the roughness of the surface (still two-dimensional but infinitely pleated) of a three-dimensional bounded domain that is densely filled by the bounded trajectories. In the normal form of the manifold (polyhedron with side-identification) this domain is $C(\Lambda) \cap \mathcal{F}$; if $\delta_H = 1$ it degenerates to a surface, in our case a "figure eight" ($\Lambda(\Gamma)$ is a circle and $C(\Lambda)$ a hemisphere).

The more the bounded tracks spread through the space the more energy is needed to move the particle into an unbounded state: If $\delta_H \to 2$ then $E_0 \to 0$, the gap between the continuous spectrum in $[\hbar^2/2mR^2, \infty]$ (cf. the end of section 2) and E_0 increases. If $\delta_H = 1$ E_0 is the only discrete eigenvalue, lying at the boundary of the continuous spectrum; an arbitrarily small amount of energy is enough to move the particle into an unbounded state, corresponding to the degeneration of $C(\Lambda)$. I also stress the fact that only the geometric shapes of the tracks count, the classical constants of motion and time serve only as formal parameters to label them, no use of Hamiltonian dynamics and phase space is made to derive (0.1). Finally I cannot resist to point out that formula (0.1) is formally not so unfamiliar as it might seem at first glance: If we choose the initial point of the interval containing the continuous spectrum as the zero point of our energy scale, or what is the same if we replace in eq. (2.1) Δ by $\Delta + 1/R^2$ (cf. the remark after eq. (2.2)), and if we write $\delta_H = 1 + 1/n$ we end up with the most elementary formula for the energy levels of the hydrogen atom (R is the Bohr radius). Note in this connection that the exterior of the Poincaré ball B^3 endowed with (2.10) is just as good a model of hyberbolic geometry as B^3 itself, and that both δ_H and $C(\Lambda)$ are determined by a discrete subgroup of the Lorentz group.

Acknowledgements

I thank N.L. Balazs, M.C. Gutzwiller, S.J. Patterson and J. Villain for special help, and B.N. Apanasov, J. Elstrodt and T. Pignataro for useful correspondence on the preprint version of this work. An exciting stay at the KFA Jülich, where parts of this work were carried out, is also acknowledged.

Note added in proof

The Hausdorff dimensions quoted in the final section have been calculated by determining the slope of $\lambda \to \log \hat{N}(\lambda)$ (cf. tables I–V) via a slightly weighted Gaussian method of least squares. The weights 1, $\log \lambda$, $\log^2 \lambda$ have been tried, the results remain unaffected by them to the accuracy given in section 8.

I would like to thank S.J. Patterson for suggesting this method. I also add the following citations: There is the impressive thesis [55] of Thea Pignataro, dealing with conformal densities (measures) on limit sets, spectral theory, quantization of geodesic flows, and all that. Here and in [56] it is shown how to express eigenfunctions as weighted integrals over classical orbits.

There are two competent reviews [53, 57], more lucid information on fundamental domains and tesselations [50, 51] and hyperbolic spaces [59–61], additional work on spectral theory and Eisenstein series [48, 52, 54, 58], and the Gelfand school [49] with the $SL(2, \mathbb{C})$ trace formula.

References

[1] W. Abikoff, Topics in the Real Analytic Theory of Teichmüller Space, Lecture Notes in Mathematics, vol. 820 (Springer, Berlin, 1980).
[2] L.V. Ahlfors, Lectures on Quasiconformal Mappings (Van Nostrand, New York, 1966).
[3] L.V. Ahlfors, Möbius Transformations in Several Dimensions, Lecture Notes (Univ. Minnesota, 1981).
[4] D.U. Anosov, Proc. Steklov Inst. Math. 90 (1967) 1; (AMS Transl., Providence, R.I., 1969).
[5] N.L. Balazs and A. Voros, Phys. Rep. 143 (1986) 109.
[6] A.F. Beardon, Am. J. Math. 88 (1966) 722.
[7] A.F. Beardon and B. Maskit, Acta Math. 132 (1974) 1.
[8] A.E. Beardon, The Geometry of Discrete Groups, Graduate Texts in Mathematics, vol. 91 (Springer, Berlin, 1983).
[9] L. Bers, Ann. Math. 91 (1970) 570.
[10] L. Bers, Bull. London Math. Soc. 4 (1972) 257.
[11] L. Bers, Bull. Am. Math. Soc. (New Series) 5 (1981) 131.
[12] L. Carleson, Selected Problems on Exceptional Sets, Van Nostrand Math. Studies, vol. 14 (1967).
[13] Y. Colin de Verdière, Ann. Inst. Fourier 32 (1982) 275; 33 (1983) 87.
[14] C.J. Earle, in: Discrete Groups and Automorphic Functions, W.J. Harvey, ed. (Academic Press, London, 1977).
[15] J. Elstrodt, Math. Ann. 203 (1973) 295; 208 (1974) 99.
[16] J. Elstrodt, F. Grunewald and J. Mennicke, Russ. Math. Surv. 38 (1983) 137.
[17] L. Ford, Automorphic Functions (Chelsea, Bronx, 1951).
[18] L. Greenberg, in: Discrete Groups and Automorphic Functions, W.J. Harvey, ed. (Academic Press, London, 1977).
[19] M.C. Gutzwiller, Phys. Rev. Lett. 45 (1980) 150.
[20] M.C. Gutzwiller, Physica D5 (1982) 183.
[21] M.C. Gutzwiller, Physica D7 (1983) 341.
[22] D.A. Hejhal, The Selberg Trace Formula for $PSL(2, \mathbb{R})$, vol. 1,2, Lecture Notes in Mathematics Nr. 548, Nr. 1001 (Springer, Berlin, 1976 and 1983).
[23] H. Huber, Comm. Math. Helv. 30 (1956) 20.

[24] S.L. Krushkal, B.N. Apanasov and N.A. Grusevskii, Kleinian Groups and Uniformization in Examples and Problems, Translations of Math. Monographs, vol. 62 (AMS, 1986).
[25] P.D. Lax and R.S. Phillips, J. Funct. Anal. 46 (1982) 280.
[26] J. Lehner, Discontinuous Groups and Automorphic Functions (AMS, Providence, R.I., 1964).
[27] W. Magnus, F. Oberhettinger and R.P. Soni, Formulas and Theorems for the Special Functions of Mathematical Physics, Grundlehren, vol. 52 (Springer, Berlin, 1966).
[28] A. Marden, Ann. Math. 99 (1974) 383.
[29] A. Marden, in: Discrete Groups and Automorphic Functions, W.J. Harvey, ed. (Academic Press, London, 1977).
[30] A. Marden, Bull. Am. Math. Soc. (New Series) 3 (1980) 1001.
[31] B. Maskit, Adv. Math. 7 (1971) 219.
[32] H.P. McKean, Comm. Pure Appl. Math. 35 (1972) 225.
[33] S.J. Patterson, Compositio Math. 31 (1975) 83; 32 (1976) 71; 33 (1977) 227.
[34] S.J. Patterson, Acta Math. 136 (1976) 241.
[35] S.J. Patterson, Math. Proc. Camb. Phil. Soc. 81 (1977) 59.
[36] D. Pedoe, A Course of Geometry (Cambridge Univ. Press, 1970).
[37] Ya.B. Pesin, Russ. Math. Surv. 32 (1977) 55.
[38] R.S. Phillips and P. Sarnak, Acta Math. 155 (1985) 173.
[39] W. Roelcke, Math. Ann. 167 (1966) 292; 168 (1967) 261.
[40] A. Selberg, J. Ind. Math. Soc. 20 (1956) 47.
[41] D. Sullivan, Publ. Math. I.H.E.S. 50 (1979) 171.
[42] D. Sullivan, Bull. Am. Math. Soc. (New Series) 6 (1982) 57.
[43] D. Sullivan, Acta Math. 153 (1984) 259.
[44] W. Thurston, The Geometry and Topology of 3-Manifolds, Lecture Notes (Princeton Univ., 1978).
[45] W. Thurston, Bull. Am. Math. Soc. (New Series) 6 (1982) 357.
[46] A.B. Venkov, Russ. Math. Surv. 34 (1979) 79.
[47] D. Wright, Oklahoma State Univ., in preparation.
[48] L.D. Faddeev, Trans. Moscow Math. Soc. 17 (1967) 357.
[49] I.M. Gelfand, M.I. Graev, I.I. Pyatetskii-Shapiro, Representation Theory and Automorphic Functions (Saunders, Philadelphia, 1969).
[50] L. Keen, Ann. of Math. 84 (1966) 404.
[51] J.W. Magnus, Non-Euclidean Tesselations and their Groups (Academic Press, New York, 1974).
[52] N. Mandouvalos, Eisenstein Series for Kleinian Groups, I.H.E.S.-preprint, 1984.
[53] S.J. Patterson, in Analytical and Geometrical Aspects of Hyperbolic Space, D.B.A. Epstein, ed., London Math. Soc. Lecture Notes 111 (Cambridge Univ. Press, London, 1987).
[54] S.J. Patterson, Mathematica Gottingensis, Heft 78, 1986.
[55] T. Pignataro, PhD-Thesis, Princeton, 1984.
[56] T. Pignataro and A.S. Wightman, in Group Theoretical Methods in Physics, Proc., W. Zachary, ed., (World Scientific, Singapore, 1984).
[57] D. Sullivan, in Aspects of Mathematics and its Applications, J.A. Barroso, ed., (Elsevier, Amsterdam, 1986).
[58] D. Hejhal, Boundary-Groups, Degenerating Riemann Surfaces and Spectral Theory, preprint, Univ. of Minnesota, 1987.
[59] B.N. Apanasov, The Geometry of Discrete Groups (Reidel, Dordrecht), to appear.
[60] D.B.A. Epstein and A. Marden, in: Analytical and Geometrical Aspects of Hyperbolic Space, London Math. Soc. Lecture Notes 111, D.B.A. Epstein, ed. (Cambridge Univ. Press, London, 1987).
[61] B.N. Apanasov, Ann. Global Anal. Geom. 6 (1988) 207.